



CHALMERS
UNIVERSITY OF TECHNOLOGY

ESTIMATION OF CUTTING FORCE BASED
ON MULTI-SENSORIAL DATA

Master Thesis Report

Jeffson Francis Kakkassery
Siragiriguhan Uthayakumar

Tuesday 22nd December, 2020

Estimation of Cutting Force based on Multi-sensorial data.
Jeffson Francis Kakkassery
Siragiriguhan Uthayakumar

Jeffson Francis Kakkassery, Siragiriguhan Uthayakumar, 2020.

Examiner: Yiannis Karayiannidis, Associate Professor,
Department of Electrical Engineering, Mechatronics Research Group,
Chalmers University of Technology, Gothenburg.

Supervisor: Stefan Cedergren, Process Engineer, GKN Aerospace Sweden AB, Trollhättan,
Sweden.

Master's Thesis 2020:09
Department of Electrical Engineering
Mechatronics Research Group
Chalmers University of Technology
SE-412 96 Goteborg
Telephone +46 31 772 1000

Cover: Estimation of Cutting Force based on Multi-sensorial data.

Jeffson Francis Kakkassery
Master thesis in Mechatronics Engineering
Embedded Electronics System Design
Department of Computer Science Engineering
Chalmers University of Technology

Siragiriguhan Uthayakumar
Master thesis in Mechatronics Engineering
Systems, Control and Mechatronics
Department of Electrical Engineering
Chalmers University of Technology

Abstract

During machining process, monitoring of cutting force is one of the important indicators which can determine different process parameters such as tool wear, the accuracy of produced parts and tool component failure. This thesis addresses an indirect approach that can measure dynamic cutting force by using multiple data from the Five-axis milling machine.

The force at the point of contact of a cutting experiment is transferred to the servo-motor with the help of ball-screws. As the force that tool exerts on the work-piece varies at every point of contact, this difference in forces is observed as a disturbance in the closed-loop controller. The controller accommodates this disturbance by providing the torque required to produce the cutting force along with the torque required to overcome the inertial and frictional forces acting on the machine. The precise estimation of the cutting force at the tool tip can be obtained by isolating the inertial and frictional torque from the motor torque provided by the controller.

The inertial and frictional torque of each feed drive is identified to derive the transfer function between the cutting force and cutting torque of each axis. As the force estimation from the transfer function is distorted and consists of the machine dynamics, a Kalman filter is used to compensate for the noises due to the dynamics of the milling machine. The cutting force estimated from the servo measurements are validated by using verification tests on each axis for the five-axis milling machine. The accuracy of the result is determined by comparing the estimated cutting force values with the force measurements from dynamometer.

The static component of the forces from the proposed model in the thesis work could not be measured due to the drift in servo-current signal measured from the CNC machine. The accuracy and similarity between the estimated forces and the measured dynamometer forces are determined by comparing the time and frequency analysis of the dynamic force measurements. It is determined from the thesis work that the dynamic component of the estimated forces are in good agreement with the measured dynamometer forces.

Preface

The master thesis work "Estimation of Cutting force based on multi-sensorial data", presents the work and research performed by Jeffson Francis Kakkassery and Siragiriguhan Uthayakumar build on the inceptive research interest of our supervisor Stefan Cedergren.

The thesis work is performed as a part of attaining academic degree for the master program at Chalmers University of Technology. The master thesis work comes under the Department of Electrical Engineering, Chalmers university of Technology and is proceeded with the guidance of Yiannis Karayiannidis who was involved in the supervision of the thesis work. The thesis report gives a brief description regarding the experimental design, the collection of the data, processing of servo-data and finally the verification of algorithm during the master thesis.

The master thesis work "Estimation of Cutting Force based on Multi-sensorial data" contains the combined description of methodologies described in various manuscripts. The thesis work addresses the design approaches and methods involved in the process of estimation of cutting force.

The thesis work was carried out completely in GKN Aerospace Trollhättan under the guidance and supervision of Stefan Cedergren, GKN Aerospace Sweden AB, Trollhättan, Sweden.

List of Abbreviations

BSFS	Ball Screw Feed System
CNC	Computer Numerical Control
BUFG	Global Buffer
FRF	Frequency Response Function
DSP	Digital Signal Processor
D/A	Digital to Analogue
PC	Personal Computer
IOT	Internet of Things
SPID	Spindle-Integrated Force Sensor
TPF	Tooth passing frequency
Fig	Figure
Hz	Hertz
rad	Radians
sec	Seconds
RMS	Root mean square
AC component	Harmonic Component
DC component	Static Component
ML	Machine learning
DH	Denavit-Hartenberg
ML	Machine Learning
CCDS	Cylindrical Capacitive
	Displacement Sensor
FFT	Fast Fourier Transformation

List of Tables

- 5.1 Frictional torque (τ_f) of each axis 25
- 5.2 Inertia (J_e) of linear (X,Y,Z) axis 26

- 11.1 Poles and zeros of the obtained transfer function X-axis. 66
- 11.2 Poles and zeros of the obtained transfer function Y-axis. 67
- 11.3 Poles and zeros of the obtained transfer function Z-axis. 68

List of Figures

1.1	Five axis representation	2
2.1	Components of cutting force during a Milling operation[1].	4
2.2	Image from the paper 'Dynamic Compensation of Spindle-Integrated Force Sensor'[2] showing sensor arrangement.	6
2.3	Schematic representation of sensors used in 'Model-based broadband estimation of cutting forces and tool vibration in milling'[3]	7
2.4	Block diagram of the proposed system	8
2.5	Axis representation of the machine	9
3.1	CNC machine linear axis Feed drive mechanism [4].	12
3.2	Block diagram of Kalman filter	15
3.3	Kistler Dynamometer [5]	16
4.1	Static load test of 20 kg on Table to determine Inertia	20
4.2	High frequency and low frequency Hammers used in hammer-test	21
4.3	Hammer test on the translational axis (X,Y and Z axis)	21
5.1	Curve Fitted Velocity-Current map of X axis	24
5.2	Curve Fitted Velocity-Current map of Y axis	24
5.3	Curve-fitting Measured Inertia in X axis	25
5.4	Curve-fitting Measured Inertia in Y axis	26
5.5	Curve-fitting Measured Inertia in Z axis	26
5.6	Estimated and Measured Torque in Y direction	27
5.7	Estimated and Measured Torque in Z direction	28
6.1	Servo-controller signals measured from CNC machine for cutting experiment	29
6.2	Variation of tooth passing frequency during cutting-test	30
6.3	Measured servo-current signal during Air-cutting test with five teeth tool .	31
6.4	Power Spectrum of measured Current signal during cutting test	32
6.5	Waterfall model consisting of individual Current signal sections	32
6.6	Variation of tooth passing frequency during cutting-test	33
6.7	Measured servo-current signal during cutting test with two teeth tool . . .	34
6.8	Power Spectrum of measured Current signal during cutting test	35
6.9	Waterfall model consisting of individual Current signal sections	35
7.1	X-axis FRF data from the hammer test	37
7.2	Y-axis FRF data from the hammer test	38
7.3	Z-axis FRF data from the hammer test	38
7.4	Block diagram of Kalman filter implementation	41
7.5	Comparison of Dynamic Air Cutting Torque of a section in X direction . .	42

8.1	Experimental Setup for validation of Cutting Force	44
8.2	Kistler dynamometer attached to table	45
8.3	Air cutting measurements from the servo-controller for X-axis	46
8.4	X-axis measurements of servo-controller for the Cutting experiment	47
8.5	Dynamometer Axis direction in comparison to CNC Axis	48
9.1	Dynamometer force of a section for each axis during Air cutting test	49
9.2	X-axis sections of servo-torque during Air-cutting experiment	50
9.3	Waterfall model of X-axis sections of Dynamometer measurement	50
9.4	Comparison between Estimated Force and Dynamometer force	51
9.5	Comparison between Estimated Force and Dynamometer force	51
9.6	Comparison between Estimated Force and Dynamometer force	52
9.7	Comparison between Estimated Force and Dynamometer force	52
9.8	Workpiece after performing two-axis cutting test	53
9.9	Measured Dynamometer Force for a particular cutting test	54
9.10	Waterfall model obtained by analysing FRF of different sections	54
9.11	Cutting torque sections of X-axis with respect to tooth passing frequency	55
9.12	Comparison between experimentally measured and estimated force	56
9.13	Comparison between experimentally measured and estimated force	56
9.14	Comparison between experimentally measured and estimated static force	57
9.15	Comparison between experimentally measured and estimated static force	57
9.16	Drift observed in estimated static force in Five teethed machining	58
9.17	Comparison between experimentally measured and estimated dynamic force	58
9.18	Comparison between experimentally measured and estimated dynamic force	59
9.19	Comparison between experimentally measured and estimated dynamic force	59
9.20	Comparison between experimentally measured and estimated dynamic force	60
9.21	Time and Power comparison between experimentally measured and estimated dynamic force	60
9.22	Comparison between Kalman estimated and Dynamometer force	61
9.23	Comparison between Kalman estimated and Dynamometer force	61
9.24	Comparison between Kalman estimated and Dynamometer force for X-axis	62
9.25	Comparison between Kalman estimated and Dynamometer force for Y-axis	62
9.26	Performance comparison before applying Kalman estimator and after Kalman estimator	63

Acknowledgement

This master thesis work was completed successfully owing to the aid and support from our supervisors, friends and families.

In full gratitude, we would like to thank our supervisor Stefan Cedergren, Process Engineer at GKN Aerospace Trollhättan for providing an invaluable opportunity to work for GKN Aerospace and for the patience, trust in our thesis work. We are extremely grateful for his time, guidance and insights throughout the master thesis work.

We thank our supervisor and examiner Yiannis Karayiannidis, Assistant Professor at Chalmers University of Technology Gothenburg for the guidance, sincere support during the period of our thesis work. We are thankful for his patience, suggestions and time until the completion of the thesis.

Also we take this opportunity to thank Chalmers University of Technology and the Department of Electrical Engineering for providing an opportunity to learn and gain experience during the period of thesis work.

We would like to express our gratitude to our Professors and colleagues for providing their suggestions and assistance during the master thesis. Finally, we would like to thank our families for their continuous motivation, encouragement and support during the tough times.

Jeffson Francis Kakkassery

Siragiriguhan Uthayakumar

December, 2020
Gothenburg, Sweden.

Contents

	i
Abstract	iii
Preface	iv
List of Abbreviations	v
Acknowledgements	ix
1 Introduction	1
1.1 Introduction	1
1.2 Five-axis milling machine	1
1.3 Thesis objective and Structure	2
2 Literature Review	4
2.1 Background	4
2.2 Approaches to determine Cutting force	5
2.2.1 Direct Estimation	5
2.2.2 Indirect measurement	7
2.2.3 Our Approach	8
2.2.4 Comparison between different approaches	10
3 Theory	11
3.1 Torque	11
3.2 Feed drive system	12
3.3 Inertia	12
3.4 Friction Models	13
3.5 Tooth Passing Frequency	14
3.6 Discrete Kalman Filter	15
3.7 Piezo-electric Dynamometer	16
3.8 Aliasing	17
4 Experimental Procedure	18
4.1 Experimental Setup	18
4.2 Design of Tests	18
4.2.1 Frictional Tests	19
4.2.2 Test for determining Inertia	19
4.2.3 Validation test for identified Inertia and Friction model	20
4.3 Hammer Test	20

5	Identification of feed drive dynamics	23
5.1	Identification of Frictional Torque	23
5.2	Identification of the Inertia	25
5.3	Identification of feed drive dynamics - Rotary drives	27
5.4	Validation of the Identified Friction and Inertia models	27
5.4.1	Discussion	28
6	Analysis of Servo Signals	29
6.1	Servo-controller Measurements	29
6.2	Analysis of Servomotor Current	30
6.2.1	Five Teeth Milling tool	30
6.2.2	Two Teeth Milling tool	33
7	Modelling of Disturbance transfer function	37
7.1	Frequency Response Function (FRF)	37
7.2	Transfer Function	39
7.3	Dynamic Modelling	39
7.4	Disturbance Model expansion	40
7.5	Implementation of Kalman Filter	41
7.5.1	Discrete Kalman Filter Design	41
7.5.2	Discussion	42
7.5.3	Filter Tuning	42
7.6	Conversion of Torque to Cutting Force	43
8	Validation Tests	44
8.1	Experimental Setup for validation	44
8.2	Validation Tests	45
8.2.1	Air cutting Experiment	46
8.2.2	Cutting Experiment	46
8.2.3	Dynamometer Measurement Setup	47
9	Results and Discussion	49
9.1	Air cutting Test	49
9.1.1	Discussion	52
9.2	Cutting Test	53
9.2.1	Static Force Comparison	56
9.2.2	Dynamic Force Comparison	58
9.3	Summary	63
10	Conclusion and Future Research	64
10.1	Suggestions for future works	65
11	Appendix	66
	Reference	72

Chapter 1

Introduction

1.1 Introduction

Manufacturing sector plays a major role in most industries to reform raw material to specific required part. In the market where mass production of material parts are required, digitizing the manufacturing process is presented as a scope to increase productivity [6]. Thus the future of the manufacturing industries will require technologies such as predictive maintenance to improve quality and to keep track on the physical data [7]. Digital Twin is the digital information of the physical system which contains all the information of the system that can be obtained from the real world. In the future the implementation of digital twin systems will facilitate manufacturing industries to achieve predictive maintenance and online-quality control during machining operations [6] [8].

The CNC machine uses cutting tool to remove excess metal in the work piece to produce parts with required specification and dimension [9]. As the heat generated during the cutting process has a significant effect on surface finish and tool's durability, several physical data including cutting force, vibration, temperature are collected during machining to predict the tool wear and also to monitor machining operations [7] [10].

The cutting force is one of the main process parameters that is to be considered to produce a work piece with good surface finish and tool life [11]. Cutting force and the surface finish are mainly dependent on the influence of feed rate and depth of cut of the tool. So, a precise control and monitoring of the cutting force is essential during machining operation as sudden change in force causes vibrations that lead to severe damage to the work-piece and machine [12] [13].

1.2 Five-axis milling machine

CNC machine uses the method of subtractive manufacturing that removes layers of metal to produce a part of the required shape, dimension. The CNC machine is a five-axis universal machining system that has three linear axes (in X, Y, and Z direction) and two rotary axes (in A and B axis) as shown in the Fig. 1.1. The number of axis of the CNC machine denotes the degrees of freedom a CNC machine can move. Servo-motors are used to control and monitor the measurement parameters of each axis of the system.

In linear axis drives, the rotary motion of the servo-motor is converted to corresponding translational motion with the help of the ball screw mechanism of the system. In rotary axis, this conversion mechanism is achieved directly from the servo-motor of the system [14] [15].

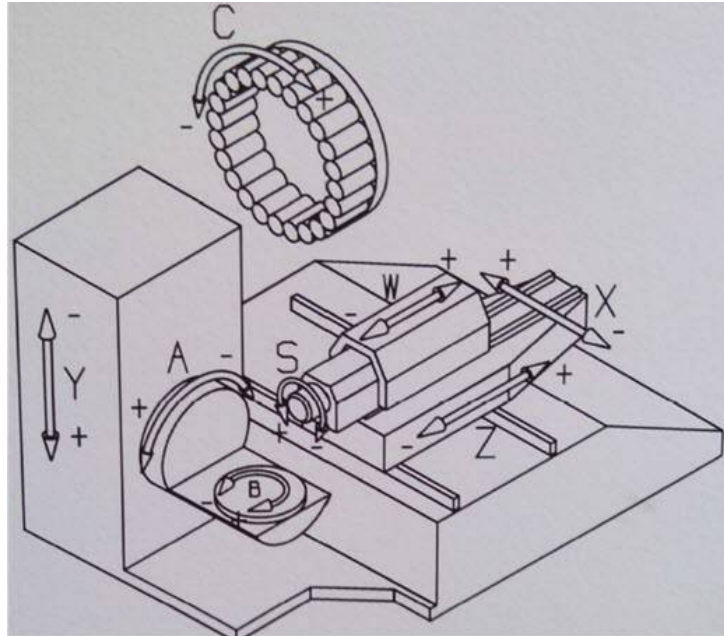


Fig. 1.1. Five axis representation

One of the important parts of a CNC machining system is the spindle and table. The spindle is located horizontally along the Z-axis and situated on the X-axis that moves linearly. The table on the other hand is resting on the Y-axis of the machine and two rotary axes A and B which also supports the table [14].

1.3 Thesis objective and Structure

The dynamic cutting force of the system is difficult to calculate mathematically and using additional sensors such as dynamometers or spindle integrated force sensors for measuring cutting forces are really expensive. Thus the primary objective of this thesis work is to establish an indirect estimation method that can estimate the cutting force for a machine that provides good bandwidth of measurements during the machining process. As dynamometers and force sensors are expensive, indirect estimation of dynamic cutting force at the tool-tip of the system is proposed by utilizing servo-controller measurements from the five-axis machine.

There are numerous approaches that are very specific to the operation mode of the machine and machine applications. After considering the approaches available for estimating dynamic cutting force, the primary focus of the thesis work is to select an ideal solution that suits best to our thesis scenario. Finally, the thesis objective is to determine an indirect method that can accurately estimate cutting forces by only using

the measurements from the servo-controller of the machine.

The master thesis is fundamentally divided into four main sections and proceeded gradually, where the first and major phase of the thesis work is the literature review that gives insight to various methodologies for estimation of dynamic cutting forces, which is presented in Chapter 2. The requirement analysis, experimental setup, and design of the experimental test for extracting the required data from the CNC controller is presented in Chapter 4. The experimental tests used in the modeling, identification of feed drive dynamics are discussed in Chapter 5. A brief analysis of the servo-signals and the frequency response is described in Chapter 6. The dynamic modeling, disturbance transfer function of the system model and implementation of Kalman filter is explained in Chapter 7. The estimated cutting force values are verified by performing machining experiments on the five-axis machine and results are discussed in Chapter 8 and Chapter 9 respectively. Finally, the conclusion and future research of the thesis are discussed in Chapter 10.

Chapter 2

Literature Review

2.1 Background

During machining process, the cutting tool rotates on its own axis and moves in the three-dimensional space along the work-piece where the cutting process occurs as shown in Fig. 2.1. The thesis work concentrates on milling operation performed by five-axis CNC machine. So the cutting force measured during the milling process mainly consists of three parts, the primary cutting force which acts in the direction of the cutting velocity, the feed force that acts in the direction of the tool feed, and the radial force that acts perpendicular to the machining surface [9]. F_x , F_y , and F_z denotes the force components during a milling operation as shown in Fig. 2.1.

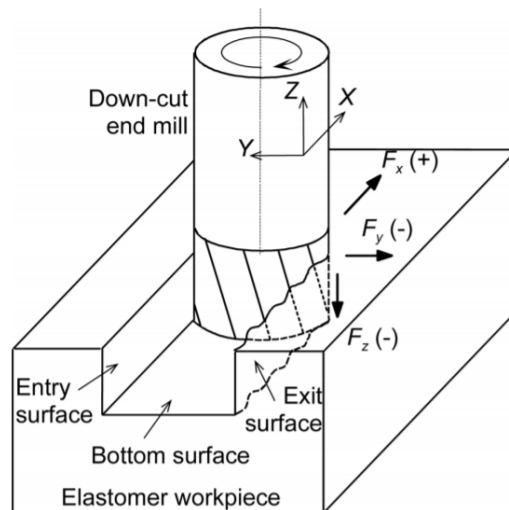


Fig. 2.1. Components of cutting force during a Milling operation[1].

The three forces shown Fig. 2.1 are F_x is the cutting force in X direction, F_y is the cutting force in Y direction, and F_z is the force in Z direction. For the milling operation shown in Fig. 2.1, F_x will have higher force values in comparison with the other force components due to the direction of milling tool [1].

The CNC machine uses a ball screw mechanism to convert the servo-motor torque to a translational force for the linear axes and a direct-drive mechanism to convert the servo-motor torque to rotational force in the case of the rotary axes. The servo-motor driving the axis has to overcome the opposing forces from the system consisting of the static and the dynamic loads of the machine. The forces due to the friction of the system contribute to both static and dynamic forces in the machine, while the dynamic forces of the system consist of forces due to inertia, acceleration, velocity, and the cutting force of the system. The dynamic and static forces of the system are balanced by the torque provided by the servo-motor. The total torque produced by the servo-motor is utilized to overcome the inertial forces, frictional force, and the cutting force of the five-axis machine.

Experimental tests are conducted which can be used extensively to determine the static and dynamic force parameters of the system. Measurements such as the commanded position, actual position, velocity, and the current of each axis can be obtained directly from the CNC machine. These measured data from the CNC machine along with the experimental tests can be used in calculating the frictional forces and the equivalent inertia of the CNC machine.

There are mainly two estimation approaches to determine the dynamic cutting forces at the tool-tip of the system. Some of the relevant estimation approaches described in various literature are reviewed in Section 2.2 to provide insight to the thesis work. Finally, Section 2.2.3 explains the estimation approach that suits best to the five-axis milling machine in the current thesis scenario.

2.2 Approaches to determine Cutting force

The estimation methods for determining the cutting force are classified into Direct estimation and Indirect estimation of the cutting force depending on the measurement from the tool-tip of the CNC machine.

2.2.1 Direct Estimation

Direct estimation of the cutting force involves measuring the cutting force directly from the tool-tip by utilizing external or internal sensors on the machine. The following literature reviewed below analyzes the advantages and disadvantages of using the direct method of estimation of cutting force.

Y. Altintas (I) and S.S. Park studied the measurement of cutting force in CNC machines which were performed by using Spindle-Integrated Force Sensors (SPIFS) mounted inside the tool. The SPIF sensors use the piezoelectric force sensor that is mounted in the spindle housing to directly measure the cutting force. Two pairs of force sensors are used to measure the shear force in the X and Y axes and a pair of compression sensors are used for Z-axis (shown in Fig 2.2). The authors obtain high accuracy by implementing a Kalman filter that could eliminate the disturbance caused by the structural dynamic model of the system [2].

Jeong-Du Kim and Dong-Sik Kim investigated the use of a dynamometer to measure the dynamic cutting force and a strain gauge to measure the static cutting force of the

system. The authors measured the dynamometer forces and implemented filters in the static force component to minimize the noise in the estimated cutting force [16].

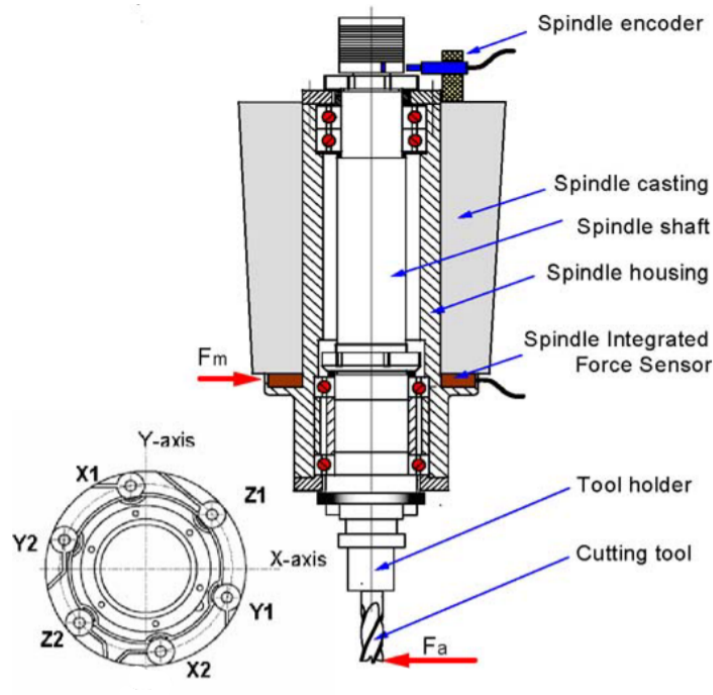


Fig. 2.2. Image from the paper 'Dynamic Compensation of Spindle-Integrated Force Sensor'[2] showing sensor arrangement.

J.H. Kim and H.K. Chang investigated the use of a Cylindrical Capacitive Displacement Sensor (CCDS) mounted on the spindle to measure the displacement of the spindle during the cutting operation. The CCDS used by the authors are highly sensitive but has lesser sensor coverage. The study shows the usage of CCDS for high-speed machining and measuring higher resolution of the cutting force [17].

Fritz Klocke and Stephan Kratz studied a method to monitor the position and force while doing the complex freeform cutting operation by using dynamometers. The study showed that the improvement in the analysis of the complex machining techniques can be achieved by the use of dynamometers [18].

Rizal and Ghani studied a direct estimation approach which is carried out with the help of a rotating dynamometer that uses a piezoelectric sensor. Similarly, Nuawi and Rizal studied a multi-sensor system using a rotating dynamometer for measuring the cutting force. The studies used an integrated rotating dynamometer and design a specified tool holder to measure cutting forces. Both the studies show the use of a rotating dynamometer for measuring the thermal effects, temperature fluctuations, and tool monitoring in the CNC system [19] [20].

By reviewing the above literature, it is observed that even though the direct measurement methodologies have higher bandwidth in the measurement of the cutting force, the

experiments require a special type of arrangement or specific sensor integrated tool to measure the cutting forces. The experiment performed by using SPIF sensor, CCDS sensors, rotating dynamometer has a high accuracy of measurement but has the limitation of high cost and requirement of specific sensor integrated tool for cutting force measurement [19] [17].

2.2.2 Indirect measurement

The indirect method for estimation of cutting forces uses external sensors or multi-sensor signals that are readily available from the CNC machine to accurately determine dynamic cutting force. It is observed that the variation of armature current in the feed drive motor depends on the load provided by the system. This principle is used for the estimation of cutting forces by the authors in various literature [21] [22]. Few authors also use an additional sensor on the tool holder to estimate the cutting forces of a CNC system [23].

Deniz Aslan and Yusuf Altintas described a method for identifying the cutting forces from the armature current measured from the axis feed drive motor. Friction, inertia, and Frequency Response Function (FRF) of the structural dynamics of each axis are identified and the cutting torque is determined by subtracting the friction and inertia from the total torque of the servo-motor. The authors also implement a Kalman filter to eliminate the disturbance caused by the structural modes of the machine. Finally, the kinematics of the machines is modeled to get accurate cutting force [24].

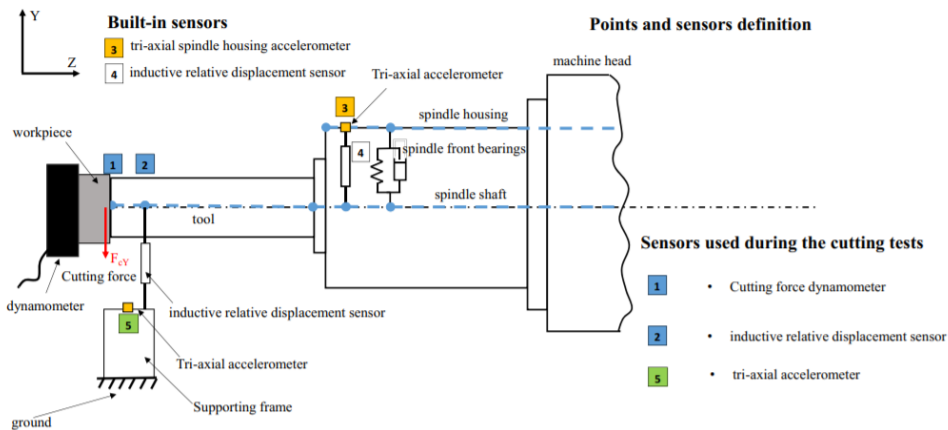


Fig. 2.3. Schematic representation of sensors used in 'Model-based broadband estimation of cutting forces and tool vibration in milling'[3]

Albertelli and Goletti used external sensors for cutting force measurement and tool condition monitoring. In this paper, an in-process model-based estimator and tool-tip vibration were designed to estimate the cutting forces. The author attached a tri-axial accelerometer which is mounted on spindle housing and an inductive sensor to measure the radial displacement of the tool. The sensor placement is shown in Fig. 2.3. The observer relies on Kalman filtering for estimating both cutting force and vibrations in the system. The study also uses sensor fusion which increases the frequency bandwidth of the

cutting force estimation [3].

Andreas, Yusuf, and Gunter explained the measurement of cutting forces by measuring the displacement of rotating spindle shafts. The paper discusses using a capacitance displacement sensor fixed into the spindle to measure the radial displacement of the rotating shaft that occurs during the cutting operation. A disturbance Kalman filter is used for the compensation of the spindle dynamics and to recover the distorted signal from the sensor. The disadvantage suggested by the author is due to temperature variation which increases flange diameter that yields the wrong cutting force [25].

The indirect approach by using servo-motor signals or attaching external sensors is used to monitor the tool condition and to accurately estimate the dynamic cutting forces of the system. Even though the sensor measurements can be compensated by using a Kalman filter, the main disadvantage of indirect estimation of the cutting force is the low bandwidth of the model when in comparison with direct estimation methods [26] [27] [25].

2.2.3 Our Approach

The literature studied above concludes that the direct estimation techniques are costly and cannot be effectively utilized while manufacturing commercial products in an industrial environment. So the method proposed in this master thesis work uses an indirect estimation technique combining the methodologies described by authors Albertelli and Goletti [3] and Deniz Aslan and Yusuf Altintas [24].

The suggested approach primarily utilizes motor drive current as well as multiple servo-controller measurements available from the CNC machine to predict the cutting forces at tool-tip of the machine. The measured data including the actual position, speed, torque, and the servo current readings are collected from each axis and are used in the indirect estimation of cutting force.

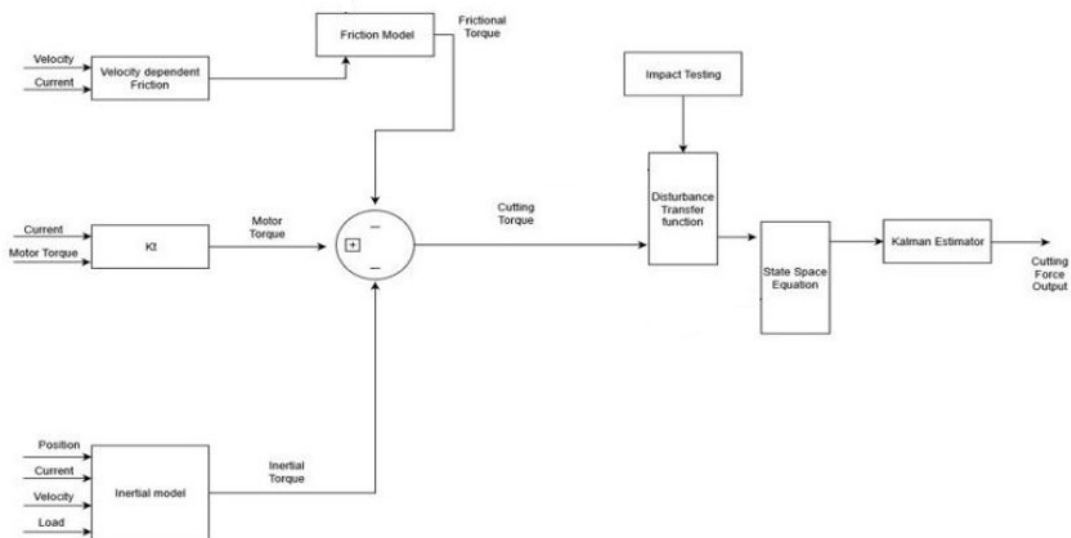


Fig. 2.4. Block diagram of the proposed system

The general proposed idea of the work is to determine the actual cutting torque during the machining process. The actual cutting torque is calculated by removing the influence of servo-torque used to overcome the feed-drive dynamics of each axis of the CNC machine. The block diagram Fig. 2.4 shows the generalized idea of the indirect estimation approach performed in the master thesis work.

Experimental machining tests are designed to determine the inertial and frictional torque of each axis. Constant velocity experiments are performed by running circular machining tests on the CNC machine to determine the feed drive dynamics of the system. The torque used to overcome the frictional forces are captured by using a suitable friction model. The inertia tests are carried out by adding known weights to measure the corresponding change in the current and torque of each axis. Finally, impact tests are performed on the CNC machine to capture the modes due to the structural dynamics of the CNC system.

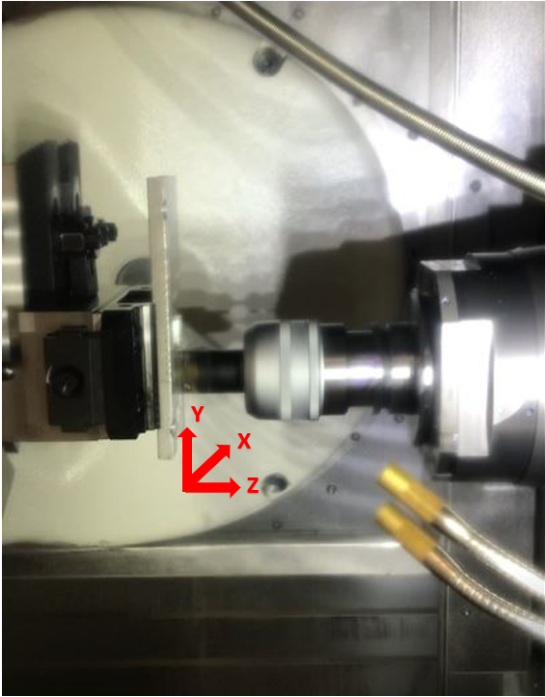


Fig. 2.5. Axis representation of the machine

The force from the impact hammer during the tests are measured and synchronized to obtain the disturbance torque for each axis. Impact force from the hammer and the corresponding disturbance torque measured from servo-drives are utilized to determine the transfer function of the CNC system. The transfer function is mapped to a state-space model and is expanded using a Kalman filter to estimate the dynamic cutting force.

2.2.4 Comparison between different approaches

Approach	Method	Sensors used	Pros	Cons
Using SPID Force sensor [2].	Direct method	Piezo-electric force sensors is used	Higher bandwidth of frequency	Special arrangement required to mount sensors.
Combined-type tool dynamometer [16].	Direct method	Strain Gauge, Piezo-film type accelerometer are used	Static and dynamic forces can be measured using two sensor	Complex signal processing, special arrangement required to mount sensors
Estimation using Spindle Displacement Sensor [17].	Indirect method	Cylindrical capacitive displacement sensor is used	Sensor has high resolution measurement of cutting force and capable of measuring high speed cutting.	Force can be measured in two axis, Sensitive to centrifugal forces.
Using Feed Drive Current signal [24].	Indirect method	Machines internal sensors are used (Servo data)	Do not require additional setup, suitable for production, good accuracy in prediction	Complex modelling, very specific, narrow approach
Using model-based tool vibration [3].	Indirect method	Accelerometer, Inductive relative displacement sensor.	Cutting force, tool tip vibration can be estimated and fused to increase bandwidth	Complex modelling, very specific, narrow approach.
Using capacitance displacement sensors [25].	Indirect method	Capacitive displacement sensor	Used for production environment.	Effect of Temperature change, Complex compensation techniques required.
Suggested approach in the Master thesis	Indirect method	Measurements from the servo-controller	Simpler approach, No additional setup required.	Lesser bandwidth, Less Accuracy.

Chapter 3

Theory

This chapter provides the theoretical background and definition to the frequently used terms with regards to the Five-axis CNC machine.

3.1 Torque

The torque of a CNC machine is defined as the measure of the dynamic rotational driving force that a servomotor can generate.

In CNC machine, the torque produced from the axial servo-motor is used to overcome the static and dynamic loads of the machine. At constant velocity, the static load of the CNC machine includes the load due to the feed drive kinematics such as friction due to the ball screw. The dynamic load of the CNC machine includes the load due to dynamic parameters such as forces due to the acceleration, velocity, and the dynamic cutting force [24]. The total torque produced by the motor can be given by,

$$\tau_m = K_t i \quad (3.1)$$

where the τ_m is the torque produces by motor, K_t is the torque constant and i is the current. The total torque generated by the servo-motor is also defined by,

$$\tau_m = J_e \alpha + \tau_f + \tau_c \quad (3.2)$$

where τ_f is the frictional torque, τ_c represents the cutting torque, J_e denotes the inertia of the axis and α represents the angular acceleration of the axis respectively.

When machining operations are carried out by a CNC machine, the cutting force at the tool-tip is reflected in the servo-motor as a disturbance torque. During the cutting operation the cutting forces are seen as disturbance in the torque values on the respective axes. So monitoring of the disturbance motor torque produced from servomotor can be used to accurately estimate the cutting force at the tool-tip of the CNC machine [24].

3.2 Feed drive system

Ball Screw Feed System (BSFS) is the transmission widely used in feed-drive system of CNC machines which provides smooth motion and low wear of feed drive by reducing the slack-slip in feed drives [4]. The feed drive system in the CNC machine uses ball screw mechanism shown in Fig. 3.1 that converts the rotational motion of the motor to the linear motion.

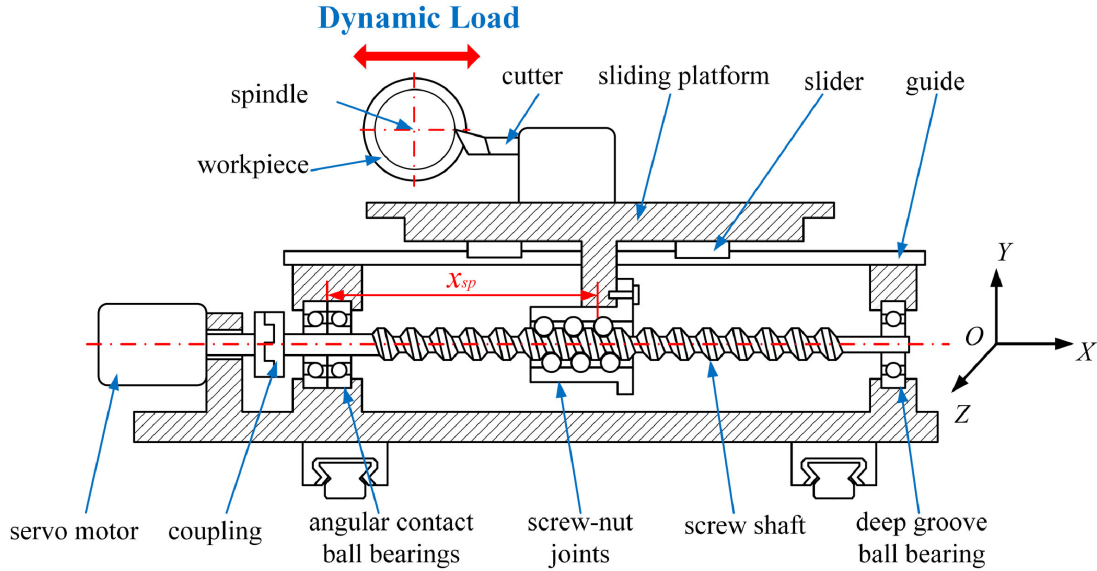


Fig. 3.1. CNC machine linear axis Feed drive mechanism [4].

The ball screw mechanism includes a screw which is assisted by bearings in the end and a nut that is attached to the table. The end of ball screw is attached to the rotary motor directly or through gear mechanism [28]. This mechanism influences the transfer of cutting force measurement from the tool to the motor with an observable disturbance in motor torque [4] [24].

3.3 Inertia

The inertia is one of the component present in the motor torque that constitutes to the dynamic load of the machine. It is required to determine inertia of each axes and subtract from the motor torque to accurately estimate the dynamic cutting force generated at the tool tip of the CNC machine [24].

The inertia of the each axis is identified using the equation given by Newtons second law of rotation.

$$\tau_{inertia} = J_e \alpha + T_{const} \quad (3.3)$$

where the $\tau_{inertia}$ is the torque in $N.m$, J_e is the moment of inertia in $kg.m^2$ and the α is the angular acceleration given in rad/s^2 and T_{const} is the constant [29].

3.4 Friction Models

Friction in general is the opposing force provided by an object when an external force is applied on it. Frictional force exists in all mechanical moving parts with contact and depends on factors such as the weight of the part, surface smoothness, area of contact between two surfaces.

To estimate the cutting force accurately, we have to eliminate the force utilized to overcome friction from the measured torque of each axis. There are various approaches to model frictional behaviour of a system. Some of the model are described below [30].

Coloumb Friction Model

Coulomb friction model can be represented by the equation

$$F = \begin{cases} F_C(Sgn(\dot{x})) & if \dot{x} \neq 0 \\ F_{app} & if \dot{x} = 0 \text{ and } F_{app} < F_C \end{cases}$$

where F_C is given by,

$$F_C = \mu F_n \quad (3.4)$$

where F is the frictional force, F_{app} is the applied force, \dot{x} is the sliding speed, F_C is the Coulomb friction, μ is the Coulomb friction coefficient and F_n is the load between two surfaces. Sgn is the sign function that denotes the \dot{x} is positive or negative with relative to the speed [30].

Viscous Friction Model

Viscous friction expresses the frictional force as linearly related to the sliding speed \dot{x} . Viscous friction model can be expressed by the equation as

$$F_V = k_v \dot{x} \quad (3.5)$$

where k_v is viscous coefficient and \dot{x} is the sliding speed [31] [30].

Integrated Coloumb and Viscous Friction Model

This model is the integration of both Coloumb and viscous model given by Andersson, Söderberg and Björklund [31] [30] incorporated the frictional force when sliding speed is closer to zero. The equation for the integrated friction and inertia model is given by,

$$F_{Int} = F_C(Sgn(V)) + F_V V \quad (3.6)$$

where V denotes the velocity of the machining, $sign$ function returns the sign of the number and F_C , F_V denotes the Coulomb and viscous friction respectively.

Stribeck Friction Model

Stribeck Friction Model can be expressed as

$$F = (F_C - (F_S - F_C)e^{(\frac{\dot{x}}{v_s})^i})Sgn(\dot{x}) + k_v \dot{x} \quad (3.7)$$

In the above equation the F represents the total Frictional force, F_C is the Coulomb friction, F_S is the static friction, v_s is the Stribeck velocity, k_v is the viscous friction coefficient, i is the exponent and \dot{x} represents the sliding speed [30].

Dahl's Model

Dahl's model of friction is used to determine the friction parameters at pre-sliding phase of a system. The model equation for Dahl's friction model is given by,

$$\frac{dF}{dx} = \sigma_0 \left(1 - \frac{F}{F_c} \text{Sgn}(\dot{x}) \right) \quad (3.8)$$

F is the Frictional force σ_0 is the stiffness coefficient and \dot{x} is the sliding speed [30].

Lugre Model

Lugre model provides a good estimate for determining frictional parameters. The equation for Lugre model is given below,

$$\begin{aligned} F &= \sigma_0 z + \sigma_1 \dot{z} + \sigma_2 \dot{x} \\ \dot{z} &= \dot{x} - \sigma_0 \frac{\dot{x}}{g(\dot{x})} z \\ g(\dot{x}) &= F_c + (F_s - F_c) e^{-\frac{\dot{x}}{v_s}^j} \end{aligned} \quad (3.9)$$

where F is the total friction force, σ_0 is the contact stiffness, z is the average deflection of the contacting blisters, σ_1 is the damping coefficient of the bristle, σ_2 is the viscous friction coefficient, x is the relative displacement, F_c is the Coulomb friction, F_s is the static friction force \dot{x} is the sliding velocity, $g(\dot{x})$ is the stribeck effect, j is the stribeck shape factor [32] [30].

3.5 Tooth Passing Frequency

During machining operations, the main constituent of cutting forces is a periodic frequency called tooth passing frequency. Tooth passing frequency is linearly dependent on the angular velocity of the spindle and the number of teeth in the tool. For milling operations where the tool contains more than one number of teeth, the tooth passing frequency is considered as a multiple of spindle speed. Depending on the stiffness of the tool, if the values of the tooth passing frequency is close to a natural frequency of the system, it results in resonance which leads to very high amplitude of vibration and chatter in CNC system [33] [34].

These high amplitude vibrations will result in instability of system during cutting process. The equation for tooth passing frequency is given by,

$$F_{Tp} = \omega N \quad (3.10)$$

where the F_{Tp} is the Tooth passing frequency, ω is the angular velocity of the cutter and N is the number of teeth in the cutter [24].

3.6 Discrete Kalman Filter

Kalman filter works as a recursive filter that calculates the current state from the previous estimated state and the current measurement. The Kalman filter is designed based on the requirements of the system. The current value of system can be accurately estimated using Kalman filter by the help of,

- The details regarding the model and dynamics of the system.
- The knowledge of uncertainty in measurement such as the disturbances in system and errors in measurement.

The transfer function observed from the system consist of the structural dynamics of the machine. So the inversion of the transfer function cannot be implemented to accurately calculate the cutting forces as it can lead to amplification of noises and instability of the system. To accurately estimate the cutting forces, the obtained transfer function is converted to a state space form. The state space representation of the system is denoted in system block of Fig. 3.2. A disturbance Kalman filter is implemented to reconstruct the actual cutting forces of the CNC system [24] [35].

The system are represented by the equations,

$$\begin{aligned} x_{k|k-1} &= Ax_{k-1|k-1} + Bu_k \\ P_{k|k-1} &= AP_{k-1|k-1}A^T + Q \end{aligned} \tag{3.11}$$

The Kalman filter for each time step $k = 1,2,3..$ is given by the equation,

$$\begin{aligned} K_k &= P_{k|k-1}C^T(CP_{k|k-1}C^T + R)^{-1} \\ x_{k|k} &= x_{k|k-1} + K_k(Tc_k - Cx_{k|k-1}) \\ P_{k|k} &= (1 - K_kC)P_{k|k-1} \end{aligned} \tag{3.12}$$

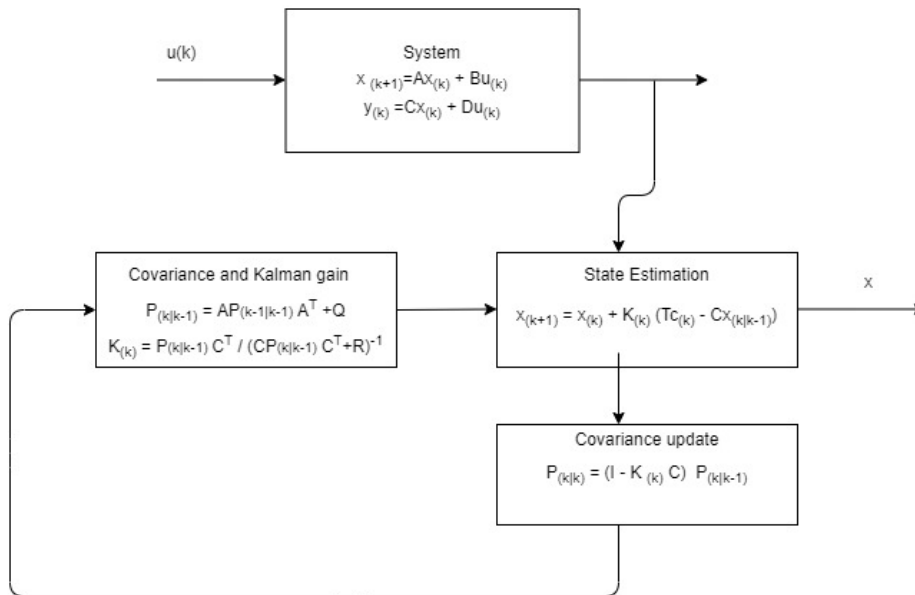


Fig. 3.2. Block diagram of Kalman filter

where A is the state matrix, B is the input matrix, C is the output matrix, Q is the system covariance matrix, K is the Kalman gain, P is the covariance matrix, R is the measurement covariance matrix, Tc is the cutting torque measurement. The state matrices (A, B, C) of the system are derived from the transfer function obtained from the frequency response function of each axis. The equation (3.11) represents the prediction step of state and covariance matrices and the equation (3.12) shows the Kalman gain calculation and update of state and co-variance matrices[36].

The predicted step is calculated based on the prior value and the model. The updated step is calculated by comparing this value to the current measurement, this iteration is carried out in a recurring manner to produce filtered output [37]. Fig. 3.2 shows the block diagram for implementation of Kalman filter.

3.7 Piezo-electric Dynamometer

The cutting forces at the tool-tip of CNC machine are measured directly by using piezo-electric dynamometers. Usually the dynamometer system is mounted on the table along with the work piece. The cutting forces are measured by the piezoelectric sensors which gives voltage output corresponding to the force measurement. The work piece on which the cutting operation takes place is mounted on top of the dynamometer.

The cutting forces varies depending on the type of material and also on the machining process. An increase in cutting speed results in decrease in the cutting force component. The measured forces using dynamometer are higher by 10 percent when milling operation is performed parallel to the rolling direction than perpendicular direction [38]. Fig. 3.3 shows a Quartz three-component dynamometer type 9257B used for the measurement of the cutting forces in a CNC system [5].



Fig. 3.3. Kistler Dynamometer [5]

3.8 Aliasing

In digital signal processing, if the frequency of the signal components in a signal is greater than the Nyquist frequency, the components are reflected back to the baseband of the signal. This is known as aliasing. Due to the effect of aliasing in signal, the signal undergoes distortions and disturbance in its harmonic property [39].

In signal processing aliasing is considered as a disturbance in signal. A signal can be reconstructed proficiently from the samples if the sampling rate is twice the maximum frequency present in the signal. Thus there is a need for applying low-pass filter or anti-aliasing filter to minimise the aliasing effect observed in the signal [40] [41]. Nyquist frequency helps us to find the maximum signal frequencies that are detectable with respect to the sampling time. Nyquist frequency can be found out using the formula,

$$F_n = \frac{1}{2t} \quad (3.13)$$

where F_n is Nyquist frequency and t is the sampling time [40].

Chapter 4

Experimental Procedure

This chapter focuses on explaining the outline of design-tests and methodology adapted to determine the friction, inertia and disturbance torque parameters of the CNC machine.

4.1 Experimental Setup

The experiments are run on a five-axis CNC machine consisting of an industrial PC, a DSP based servo-controller, motorised spindles and servomotors for each axis. The measured signals are sent to encoder which consist of a 64-bit as well as a 32-bit D/A converter in the DSP system.

The five axis CNC machining essentially consists of a moving part and three axis drives, where the movement of each axis is controlled by a servo-controller as seen in the Fig. 1.1. Referring to Fig. 1.1, the Y axis drive of the machine supports both the A and B axis (rotary axes) of the milling machine. The support of the rotary axes by the Y-axis induces a deviation both in rotary and Y axis measurement while operating the CNC machine. This deviation can be observed plotting and comparing the Y-axis servo measurement with the other linear axis. The X and Z axis drives of the CNC machine are independent of other axis [14].

4.2 Design of Tests

The total motor torque of the feed-drive system consists of the torque used to overcome the frictional, inertial forces and also the cutting torque which is exerted by the tool on work-piece. So the total motor torque of the feed-drive system can be represented by the equation (3.2). So to accurately estimate the cutting torque (τ_c) exerted by the feed-drive system, it is required to have an accurate measurement of the frictional torque τ_f and torque due to inertia ($J_e\alpha$).

The purpose of the experimental tests design is to utilize the velocity, position and torque measurements from the servo-controller of the five-axis milling machine, to determine the friction, inertia and disturbance torque parameters of the CNC machine.

4.2.1 Frictional Tests

Friction is the resistance to the motion of the system relating to nearby surfaces (see section 3.3). The friction of a CNC machine depends on various factors including the temperature of the surroundings, the surface of the material, the dimension of the ball screw and the feed drive velocity.

The frictional torque experiments of the CNC machine is designed by moving the table part of the CNC machine and measuring the corresponding position and torque values from the encoders of the CNC machine. A constant velocity experiment is performed to measure the frictional torque in the CNC machine.

Constant Velocity Experiment

The velocity-dependent friction is estimated by performing a constant velocity experiment for each axis of the five-axis milling machine. The test is used for determining the effect that varying feed-drive velocity has on the frictional torque of each axis. Before running the experiments, the servomotor is switched to the position control loop and is warmed up for a few minutes to avoid the dwell time effect.

After avoiding the dwell time measurements, the CNC is operated in the position control loop which results in each position commands to move the CNC machine table. The table is moved in order of a ramp signal so as to produce a constant velocity while moving from position A to position B and a negative ramp of same intensity which moves the table back to position A. The test is repeated with different positional ramp slopes and is averaged to find the averaged velocity-dependent friction of the CNC machine [42].

4.2.2 Test for determining Inertia

Along with the friction forces, the motor torque of each axis is also dependent on the inertia forces of each axis. The torque due to inertia of each axis of the CNC machine is estimated by loading the CNC machine with known weights considering the initial torque set point of each axis. Weights of 25 kg, 20 kg, 10 kg, 5 kg, 2.5 kg, 0.5 kg are loaded on each axis to observe and determine the effect of inertia on the motor torque.

Static Load on Linear and Rotary Axis

In order to determine the torque due to inertia on the linear and rotary axis, a static loading experiment is performed on the linear and rotary drives of the five-axis milling machine.

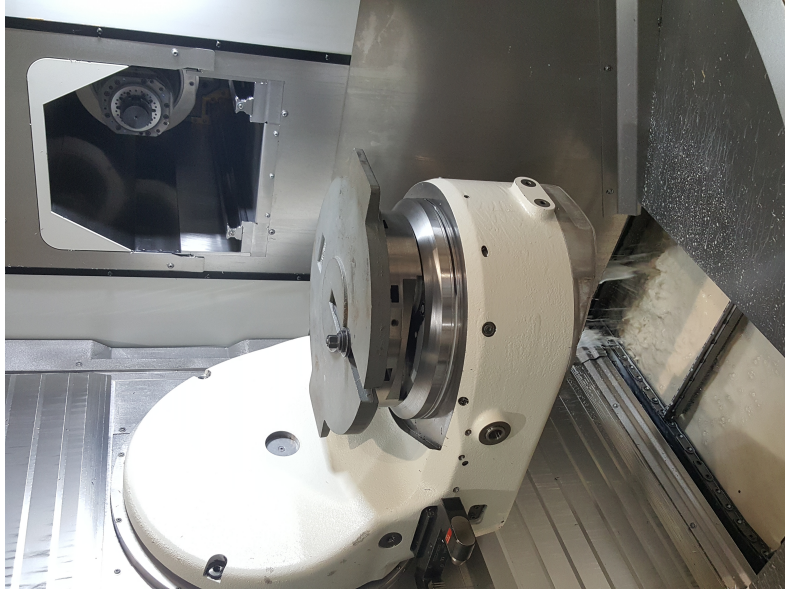


Fig. 4.1. Static load test of 20 kg on Table to determine Inertia

Fig. 4.1 shows experimental setup of the CNC system to determine the Inertia. Static loading of the drives is performed by positioning the weights on the table and measuring the corresponding disturbance torque from the servo-motor. The servomotor is switched to the torque control loop and is warmed up before running the tests to remove the dwell time effect of the CNC machine. Each drives are loaded with weights progressively and the corresponding servomotor current and position readings are measured continuously. The experiments are repeated and averaged to find out the average inertia in each direction.

4.2.3 Validation test for identified Inertia and Friction model

Validation tests are performed in each axis to determine the accuracy and correctness of the identified friction and inertial model. The accuracy of the developed model is observed by comparing the measurements from the estimated model to the actual readings from the five-axis system.

The servomotor is switched to the torque control loop and is warmed up before running the tests to remove the dwell time effect of the CNC machine. The validation tests are conducted by running the moving part (CNC table) of the system in circles with increasing steps of velocity. The corresponding servomotor measurements are recorded for the validation of the friction and inertia of the milling system.

4.3 Hammer Test

Hammer or Impulse tests are performed on each axis drives to capture the behaviour of the feed-drive dynamics of each axis. As mentioned in previous section, the dynamic cutting force at the tool-tip is observed as disruption in the servo-controller, this disturbance in the servo-controller is captured by performing a hammer test or impulse test on the machine. Low and High frequency instrumental hammers (see Fig. 4.2) are used to excite

the machine parts and feed-drives to a range of frequencies, as shown in Fig. 4.3.



Fig. 4.2. High frequency and low frequency Hammers used in hammer-test

As seen in Fig. 4.3, the spindle of the machine is struck with different force pulses in directions to the linear drives (X, Y and Z axis) and rotary drives (A and B axis).The hammer force and the response torque from the servo-motor are of different sampling rate and are measured using an external data acquisition system.

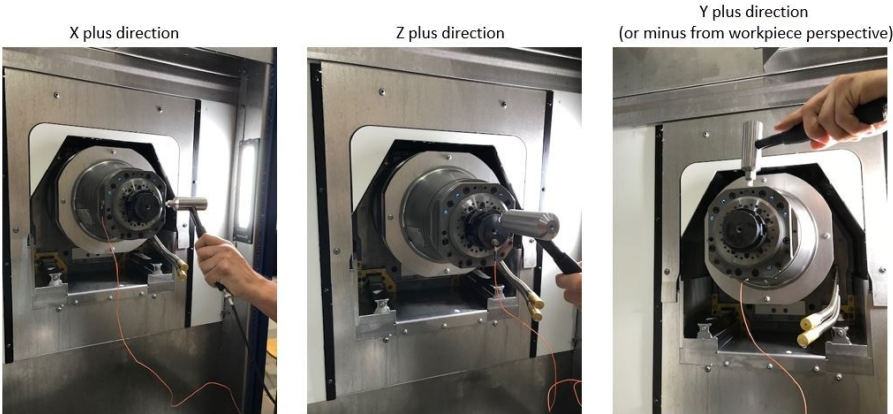


Fig. 4.3. Hammer test on the translational axis (X,Y and Z axis)

The response torque from the servo-controller during hammer test is used for developing a black-box transfer function between the servomotor torque and dynamic cutting force. To

determine the transfer function, Fast Fourier Transformation (FFT) is used to transform the hammer force and the response servo-torque into frequency domain.

$$\tau_f(j\omega) = \frac{1}{2\pi} \left\{ \int_0^{\infty} 2f(\omega)e^{i\omega t} d\omega \right\} \quad (4.1)$$

$$\tau_a(j\omega) = \frac{1}{2\pi} \left\{ \int_0^{\infty} 2\tau(\omega)e^{i\omega t} d\omega \right\} \quad (4.2)$$

where τ_f is the hammer force converted to torque, ω is the angular frequency, τ_a is the torque from the CNC, T is the sampling time of the CNC system. The transfer function of the system is obtained by dividing FFT of servo-torque (equation (4.2)) by FFT of the hammer force (equation (4.1)).

$$\Phi_{d(s)} = \frac{\tau_f(j\omega)}{\tau_a(j\omega)} \quad (4.3)$$

where $\Phi_{d(s)}$ denotes transfer function of the system. The $\Phi_{d(s)}$ of each axis is calculated by averaging the response obtained while applying repeated force on each axis of the CNC machine (see Fig. 4.3).

Chapter 5

Identification of feed drive dynamics

This chapter focuses on the brief discussion of observed results from the friction and inertia tests performed on the five-axis milling machine.

5.1 Identification of Frictional Torque

The torque utilized in overcoming the frictional force is required to determine accurate estimation of the cutting torque. To calculate the effect of velocity dependent frictional forces acting on the system, constant velocity experiments (Section 4.2) was performed in each axis. The frictional behaviour of the linear axis of the system can be calculated from the equation (3.2).

During an air cutting experiment, no torque is expended on cutting forces at tool-tip. Then the observed motor torque (τ_m) is only the summation of the torque required to overcome inertia of the feed-drive system and the frictional forces. So the equation (3.2) can be rewritten as,

$$\tau_m = J_e \alpha + \tau_f \quad (5.1)$$

As mentioned in previous section, the air-cutting experiments of the Five-axis milling system are performed in constant velocity (see Section 4.2). During a constant velocity experiment the angular acceleration of the system is determined to be zero. Thus the total motor torque utilized during a constant velocity air cutting experiment is entirely used to overcome the frictional forces of the axis. So the equation (5.1) can be re-written as

$$\tau_m = \tau_f \quad (5.2)$$

In course of a steady state motion of the machine, the velocity dependent friction can be obtained by measuring the motor torque from the servo-controller. As the frictional parameters of a system are velocity-dependent, the dependency between the frictional torque and the velocity can be captured by producing a velocity-friction mapping shown in figure.

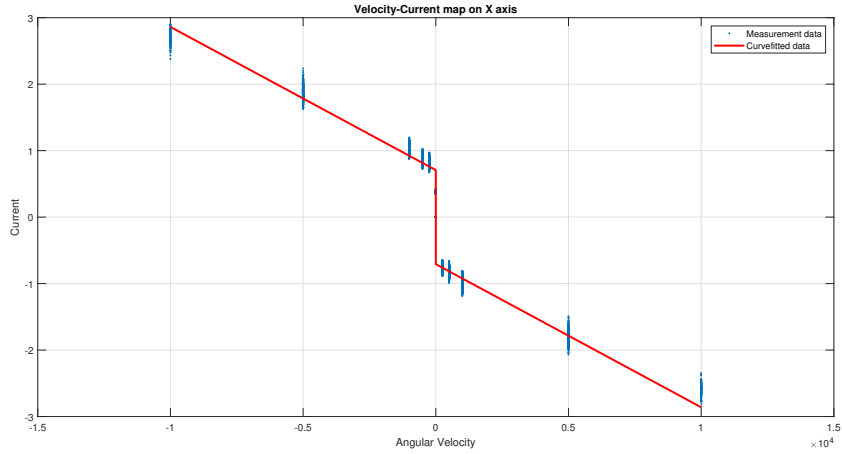


Fig. 5.1. Curve Fitted Velocity-Current map of X axis

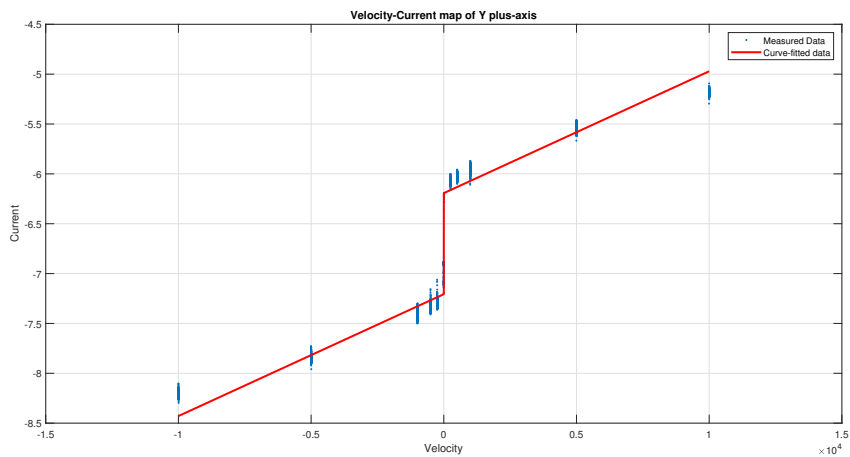


Fig. 5.2. Curve Fitted Velocity-Current map of Y axis

Velocity dependent friction parameters of a system can be determined by utilizing linear curve fitting method on appropriate friction model.

Discussion

From Fig. 5.2 we were able to observe the absence of Stribeck effect as well as the absence of static friction on the velocity-torque map. This summarised the exclusion of dynamic parameters of the friction on the system. The modelling of the frictional parameters of the five-axis machine is settled by using a Viscous and Coulomb model of friction. This is represented by the equation (3.6). The table shows the identified frictional values for linear axis.

The proposed friction model does not detect the frictional torque when velocity approaches zero. As the friction model (refer Fig. 5.2), could not capture the friction

parameters at very low velocities (Zero friction), the proposed model appears to have a pseudo static friction when velocity approaches to zero.

Table 5.1: Frictional torque (τ_f) of each axis

Axis	Coulomb Friction	Viscous friction
X-axis	-1.52	-4.63*e-04
Y-axis	1.09	2.63*e-04
Z-axis	-1.58	-3.07*e-04

5.2 Identification of the Inertia

Beside the effect of frictional forces, the identification of the cutting force generated at the tool-tip of the CNC machine requires the estimation of the torque utilized to overcome the inertial forces inside the system. The inertial test are performed to determine the static load inertia in linear axis of the Five-axis milling (see Section 4.2.2).

In inertial tests, a static load is used to determine the alteration between the axial load and the servo torque. This translation of the axial load is then compared to the dynamic test on the five axis machine to obtain the inertia of each direction of the drives. The inertia due to mass loaded on the system is provided by the equation (3.3).

It can be determined from equation (3.3) that the maximum inertial torque arises when the load is being accelerated. The inertia J_e and constant torque T_{const} is calculated to model the torque required in overcoming the inertia of each axis.

Thus the inertia of each axis is determined by curve fitting the motor torque measured after deduction of the torque needed to overcome the frictional forces shown in equation (5.1),

$$J_e \alpha = \tau_m - \tau_f \quad (5.3)$$

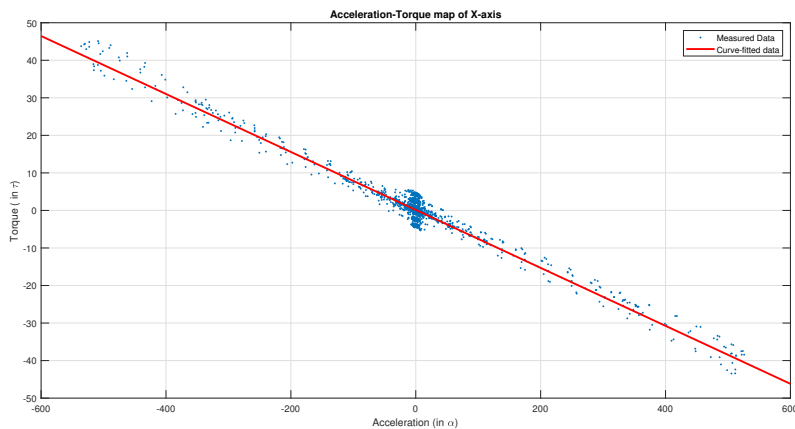


Fig. 5.3. Curve-fitting Measured Inertia in X axis

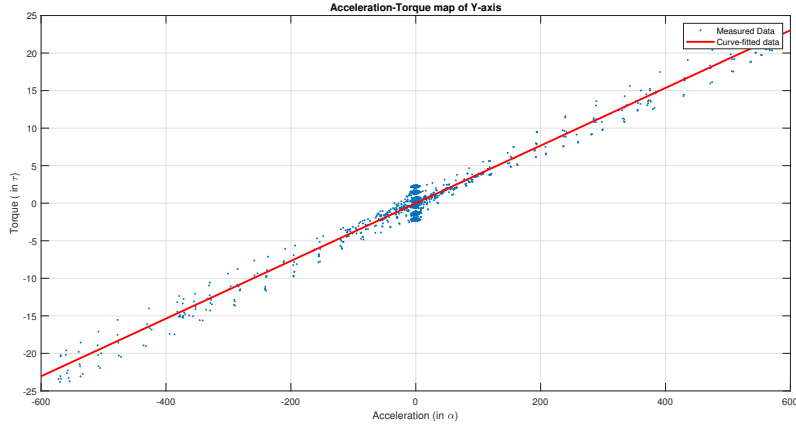


Fig. 5.4. Curve-fitting Measured Inertia in Y axis

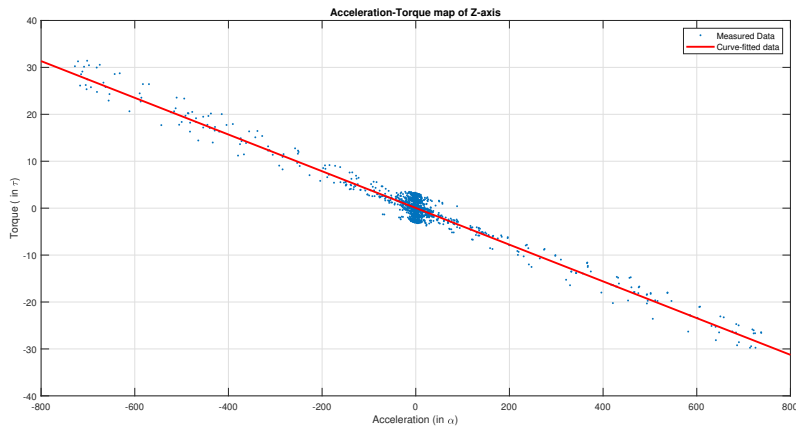


Fig. 5.5. Curve-fitting Measured Inertia in Z axis

Fig. 5.5 shows the curve fitted curves in the identification of inertia in translational axis. The graphs of the translational axis's shows a linear relation between Inertia and feed-acceleration. The inertial parameters identified from the curve fitting for the system is shown in Table 5.2.

Table 5.2: Inertia (J_e) of linear (X,Y,Z) axis

Axis	Inertia (J_e) of the system	T_{const}
X-axis	0.00772	0.1372
Y-axis	0.00385	0.0140
Z-axis	0.00391	0.0427

The Table 5.2 shows the identified inertia values for each direction of linear axis.

5.3 Identification of feed drive dynamics - Rotary drives

To determine the feed drive dynamics of the rotary axis of the CNC machine static load tests are performed on the A and C drives. The difference in behaviour of the rotary axis in comparison to the the linear drives are due to the direct drive mechanism in the rotary system. The feed drive dynamics of the system is determined by performing static load test on the rotary axes.

The FRF of the rotary axis shows high stiffness, this response behaviour of the system can be credited due to the uncertain behaviour of the axis. The rotary axis A and C drives are not taken into account while performing cutting operation.

5.4 Validation of the Identified Friction and Inertia models

To determine the accuracy and correctness of the identified friction and inertia models, validation tests are performed in each linear axis of the Five-axis milling machine (see section 4.2.3). The torque readings from the servo-controller is analyzed with respect to the estimated torque from the friction and inertia models. Fig. 5.6 and Fig. 5.7 shows the measured torque from the system and the estimated torque.

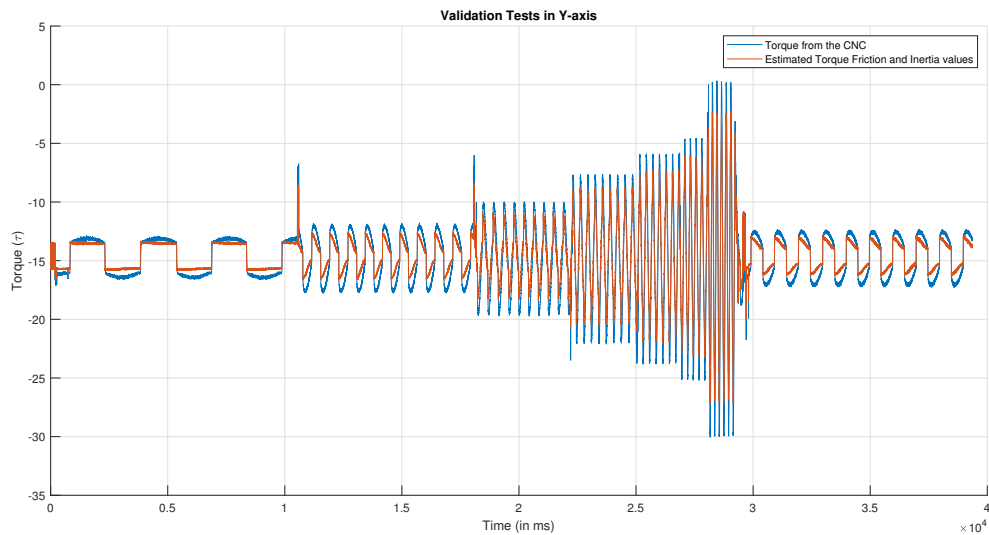


Fig. 5.6. Estimated and Measured Torque in Y direction

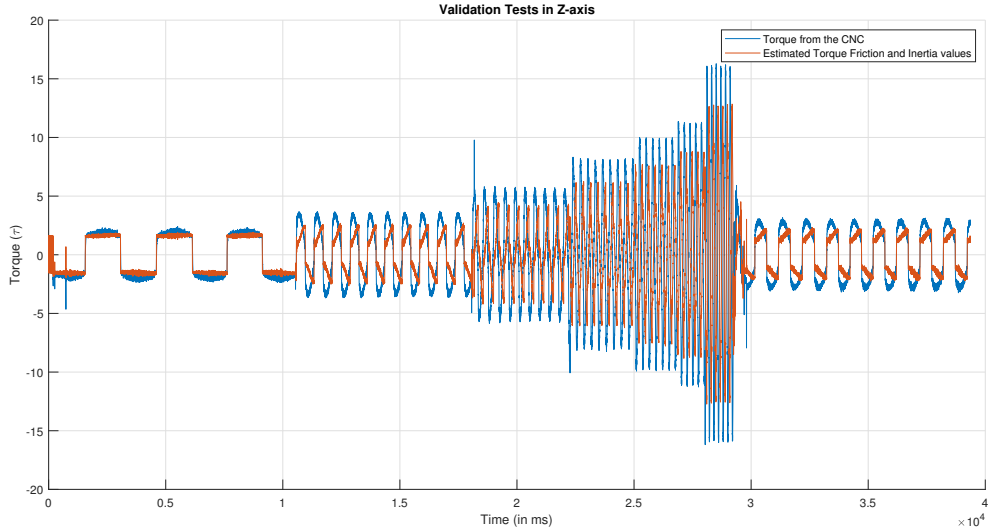


Fig. 5.7. Estimated and Measured Torque in Z direction

5.4.1 Discussion

From Fig. 5.7 we could observe the estimated model follows the measurement data at low velocity circles. During high speed machining it can be observed that the estimated torque is clipped and does not follow a smooth curve transition as observed in the measured torque. This can be attributed to the presence of the Stribeck effect of friction at higher velocities of operation. Thus it can be concluded that the Coulomb and viscous friction model utilized in the thesis work does not accurately capture the influence of friction during higher velocities due to the presence of Stribeck effect.

The proposed friction model does not accurately estimate the cutting torque when cutting torque is lesser than the frictional torque. This imprecise estimation can be observed while performing air cutting experiments on the CNC machine. The total cutting torque exerted by the servo-motor during air cutting is zero, but the proposed friction and inertia model provides a pseudo-static frictional force at very low velocities (closer to zero). During an air cutting experiment the system, the system estimates to have a low pseudo-frictional torque.

A low to high speed grade machining tests are conducted to analyse the the structural dynamics of the CNC system. The accuracy of inertia and friction model plays a major role in capturing accurate feed-drive dynamics of the CNC system. The accuracy of friction and inertia model proposed in the master thesis is greater during low spindle velocity than at higher velocities, thus a low spindle speed machining tests are prioritised to analyse and verify the proposed system.

Chapter 6

Analysis of Servo Signals

The chapter focuses on the analysis of servo-controller measurements and also provides a brief discussion on selection of tool to smoothly estimate the cutting force during machining process.

6.1 Servo-controller Measurements

The servo-controller measurements can be used to control the machining process and also provides information regarding the CNC system during the process. The servo-controller signals measured from the internal sensors of the five-axis CNC machine consists of the actual position reading, the load, servomotor current, commanded torque, spindle speed and velocity measurements as shown in the Fig. 6.1.

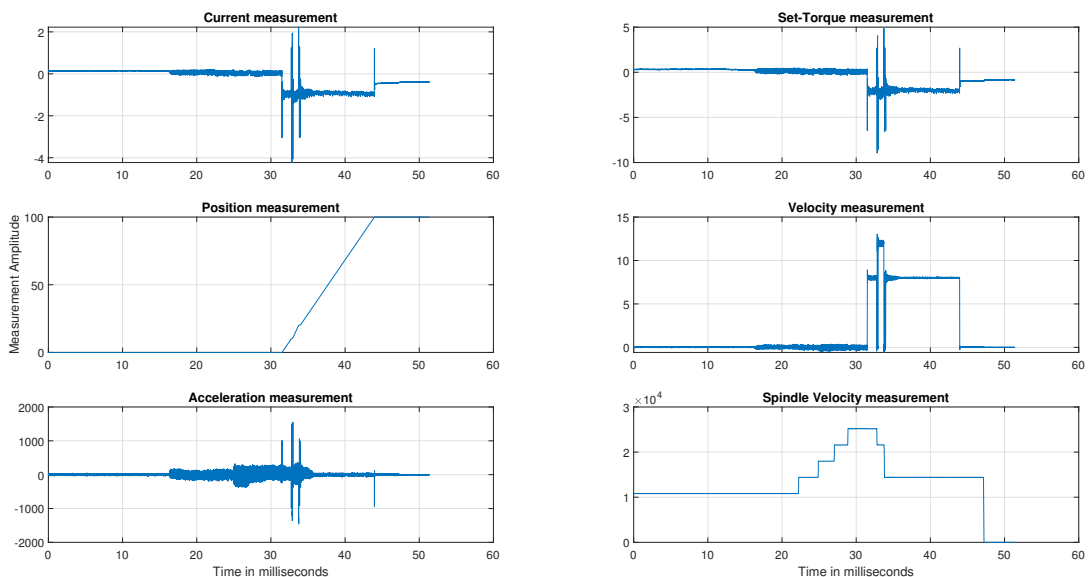


Fig. 6.1. Servo-controller signals measured from CNC machine for cutting experiment

The servomotor current and the set torque measurements from the five axis milling machine are used to estimate the cutting force exerted by the tool-tip of the machine.

6.2 Analysis of Servomotor Current

The current signal from the servo-controller is used to estimate the cutting force of the CNC machine. The servo-signals are analysed to provide information regarding the influence of tooth passing frequency on cutting process of the CNC machine. To observe this influence, machining tests are performed with high spindle speed and low spindle speed with the aid of five teeth tool and two teeth milling tool.

6.2.1 Five Teeth Milling tool

The CNC machining process is performed via five-teeth milling tool to observe the influence of the tooth passing frequency on the cutting forces.

The tooth passing frequency observed from the machine is dependent on the spindle speed and on the number of teeth of the milling tool (refer Section 3.5). Using the equation (3.10), the relation between spindle speed and the tooth passing frequency for a five teeth milling tool is shown in Fig. 6.2.

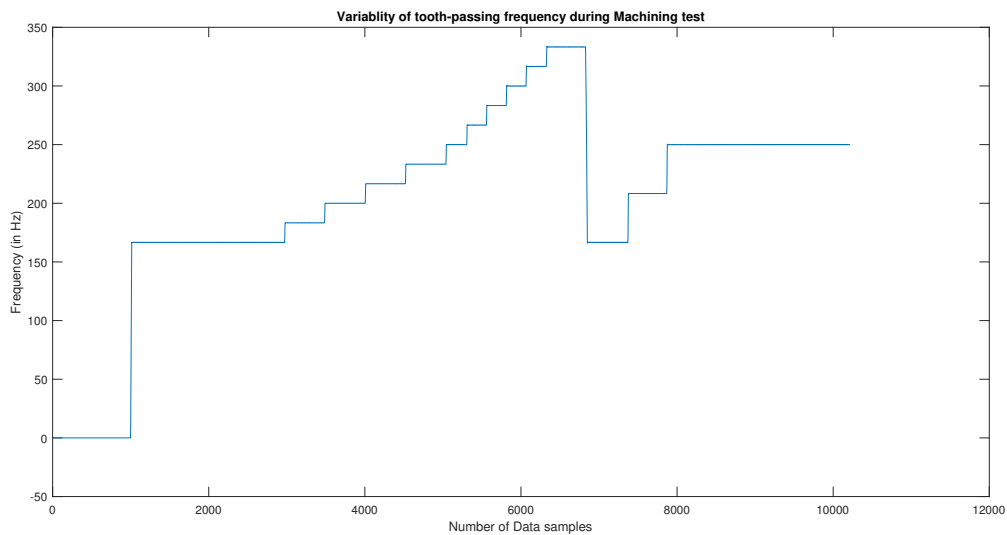


Fig. 6.2. Variation of tooth passing frequency during cutting-test

The disturbance caused due to spindle speed can be observed as tooth passing frequency in the servo-motor signals. From Fig. 6.2, it can be observed that the tooth passing frequency increases as the spindle speed increases. As tooth-passing frequency causes distortion in the servo-motor signals, it can be averted by proposing a model for tooth passing frequency of the system (refer Section 7.4). The tooth passing frequency, can be illustrated by a periodic disturbance noise. A *sine* function or *cosine* function can be used to model this periodic disturbance noise in the system.

To analyze the influence of machining speed and number of teeth of tool over tooth passing frequency, a low to high spindle speed machining tests are performed on our system using a five teeth milling tool.

Speed-varying machining Test

Variable speed test is conducted by increasing the machining speed of the spindle from low frequency to high frequency.

The speed-varying machining test is performed over the CNC machine to observe the effect of spindle speed and the forced vibrations on the measured servo-signals. The current signal measured from the speed varying machining test is shown below in Fig. 6.3.

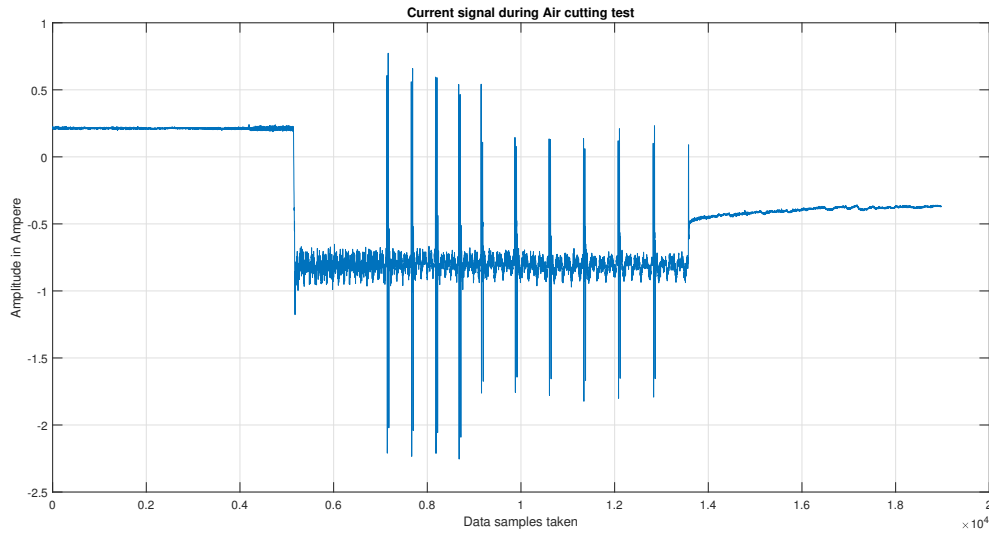


Fig. 6.3. Measured servo-current signal during Air-cutting test with five teeth tool

The current measurements from the servomotor (Fig. 6.3) consist of the low and high speed machining, with an initial data offset of 0.3 A.

During the variable test it is observed that the spindle starts at samples 1200, but the movements are not noticeable in the current measurements. So it can be concluded that the measured current signal from the servo-motor captures the machining process but the low frequency spindle movements during the variable speed test is not reflected in the servo-motor current. At the end of machining tests it can be noted that the servo-current remains at an offset of -0.4 A rather than reverting to zero current. The offset can be attributed to the deviation in ball screw position of CNC machine.

Power Spectrum of Current signal

The current measurement from the servomotor system consists of N samples with an indefinite sampling rate of 250 Hz. The power spectrum of the time domain signal provides information regarding the signal power in the system [43]. The influence of the tooth passing vibrations on the system is reflected in the current signal (all servo-motor signals). To observe the influence of tooth passing vibrations and the distortions in signal, power spectral density of the current signal is analysed. Fig. 6.4 shows the power spectrum of the servo-current signal.

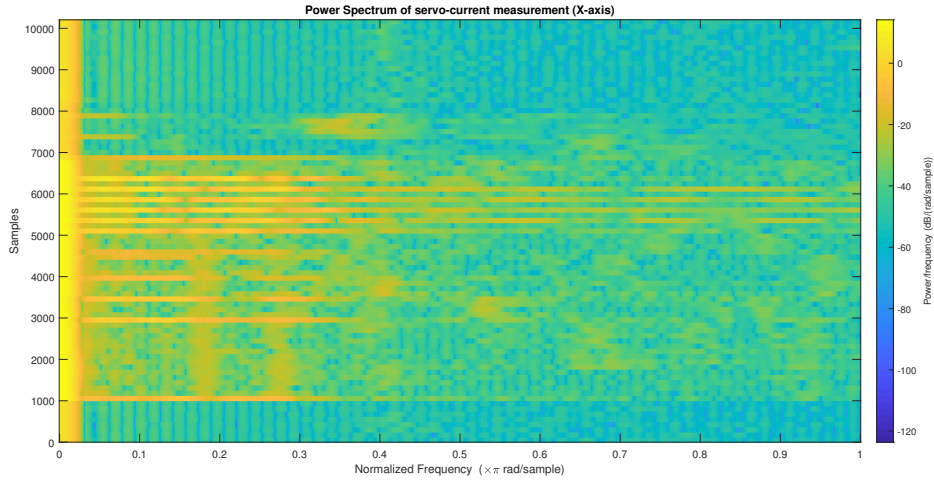


Fig. 6.4. Power Spectrum of measured Current signal during cutting test

The power spectrum of the current signal shown in Fig. 6.4, provides data regarding the difference in power with respect to varying steps of machining speed (similar to Fig. 6.2). After analyzing the spectrum, it can be observed that the power spectrum provides insufficient information on the effects of tooth passing frequency due to the overlapping between adjacent steps and also due to the lower resolution of the spectrum. These inaccuracies of the power spectral analysis can be minimized by splitting the servo-current signal into smaller sections based on tooth passing frequency and plotting a waterfall model.

Waterfall model of Current signal

The current measurements from the servomotor consist of unwanted disturbances and overlapping. To reduce the inaccuracies, the signal is divided into different sections based on the tooth passing frequency. Fig. 6.5 shows the waterfall model containing frequency response generated from each section of the current signal.

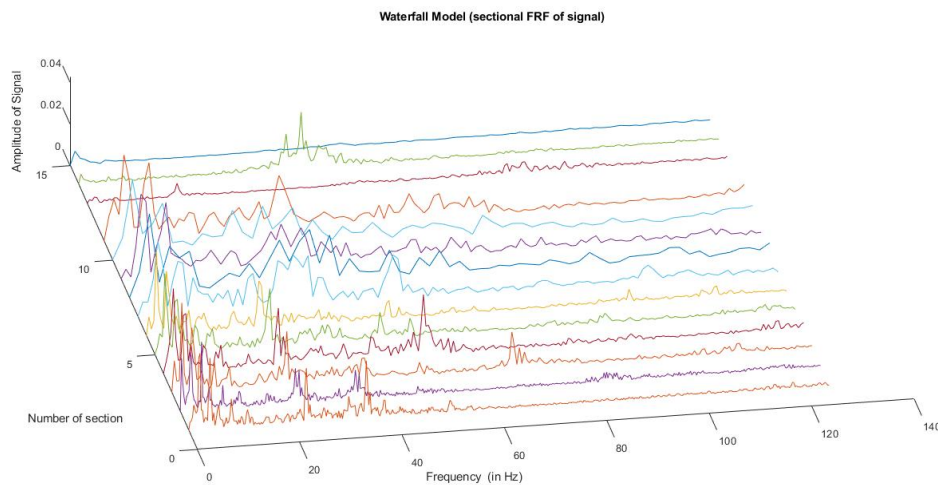


Fig. 6.5. Waterfall model consisting of individual Current signal sections

By examining the waterfall model (Fig. 6.5) it can be observed that the servo-current signal is noisy and provides very little information on the effect of the tooth passing frequency on the servomotor signal. One of the major reasons for the noise in each frequency response data of each signal section is due to the variable sampling rate (around 250 Hz) of the servo-motor signal. As the signal information lost in certain periods of time, the signal is reconstructed (using *fillmissing* function in MATLAB) which increases the disturbance in the signal. Another major reason for the noises observed in the waterfall model is due to aliasing between the signal frequencies.

Discussion

The tooth passing frequency of the cutting test using five teeth tool is shown in Fig. 6.2. The power spectrum and the waterfall model of the signal do not capture the influence of tooth passing vibrations generated from the tool-tip due to the disturbances in the signal. One of the major disturbance is caused by the tooth passing frequency (see Fig. 6.2) higher than Nyquist sampling rate (125 Hz). The system does not satisfy the Nyquist stability criterion (see Section 3.8) leading to aliasing in the signal. Another major reason for the disturbances is due to the variable sampling rate of the signal and noises induced during the manual reconstruction of the signal (*fillmissing* in MATLAB).

The tooth passing frequency depends on spindle speed and the number of teeth of the tool (see equation (3.10)). The tooth passing frequency of CNC machine can be decreased when the machining process is restricted to lower number of tool teeth and low spindle speed machining. To observe and capture the desired tool vibrations, the tests are repeated with two teeth milling tool at slow spindle speed.

6.2.2 Two Teeth Milling tool

The machining experiment is repeated with a two teeth milling tool to reduce the influence of aliasing observed during the five teeth milling machining. To analyze the frequencies present in the current measurements, low spindle speed tests are performed on the CNC machine.

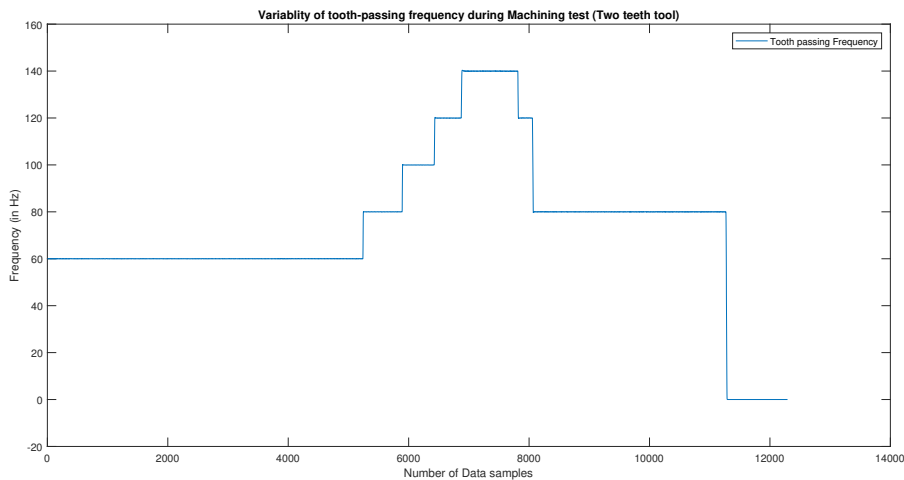


Fig. 6.6. Variation of tooth passing frequency during cutting-test

The relationship between the tooth passing frequency and varying spindle speed is given in Fig. 6.6. As discussed before, the spindle velocity and the number of teeth of the tool influences the tooth passing frequency (see equation (3.10)). When number of teeth is decreased, it is reflected in the system as a decrease in the tooth passing frequency, bringing the tooth passing disturbances closer to Nyquist sampling rate (125 Hz). So lowering the parameters reduces the effects of aliasing in the servo-signal. The difference can be observed by comparing the tooth passing frequency of the five teeth tool (Fig. 6.2) with two teeth tool (Fig. 6.6).

Low speed machining test

A low spindle speed machining test is performed on the CNC machine to capture the effects of tooth passing frequency in the system. The servo-current measurement during the low speed grade machining is given in Fig. 6.7.

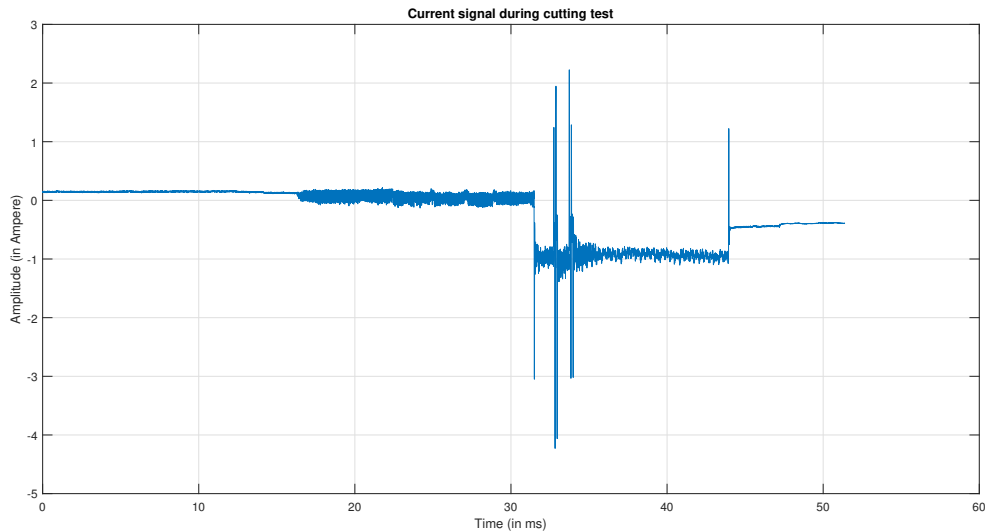


Fig. 6.7. Measured servo-current signal during cutting test with two teeth tool

The tests are designed with low speed spindle speed to reduce the effects of aliasing in the system as observed in five teeth tests. We can observe that the servo-motor current signal (Fig. 6.7) starts with an offset of 0.2A from zero. This offset at start and end of the servo-current signal can be attributed to the deviation in ball screw position of the feed drive system.

Power spectrum of Current signal

Power spectrum provides information regarding the distribution of power among the different frequencies of the signal [43]. The power spectrum of the current signal while performing a low grade speed test is shown in Fig. 6.8.

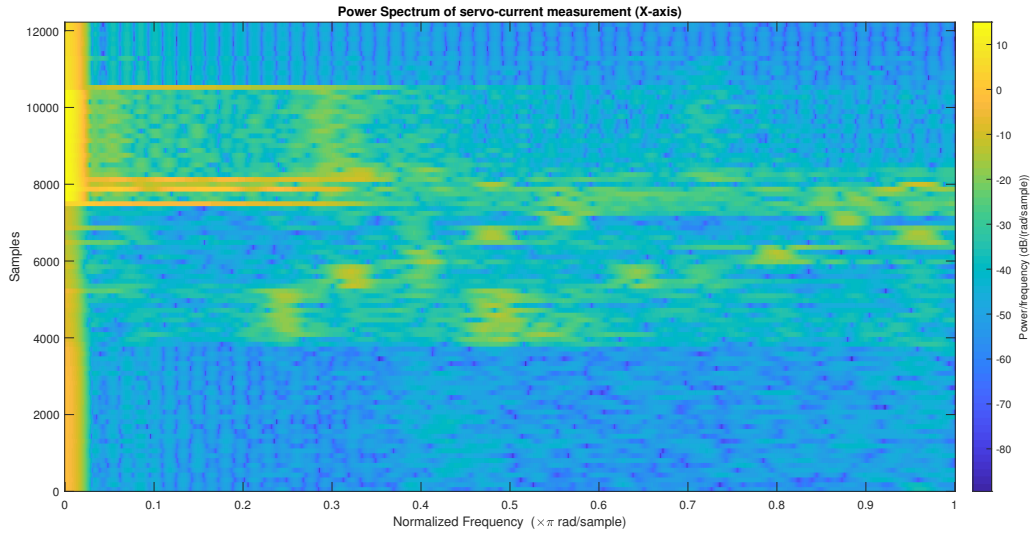


Fig. 6.8. Power Spectrum of measured Current signal during cutting test

From the spectrum Fig. 6.8 shows the distribution of power at different frequency ranges of the current signal. The change in power due to the tooth passing frequency can be observed from the power spectrum of current signal. Comparing the tooth passing frequency identified from spectrum it can be observed that the spectrum follows the tooth passing frequency identified theoretically as shown in Fig. 6.6.

Waterfall model of Current signal

As the current measurements consist of overlapping and unwanted disturbances, the signal is divided into various sections which are averaged in mean to reduce the static offset observed in the signal (Fig. 6.7). Fig. 6.9 shows the waterfall model consisting of frequency response data generated from each section of the current signal.

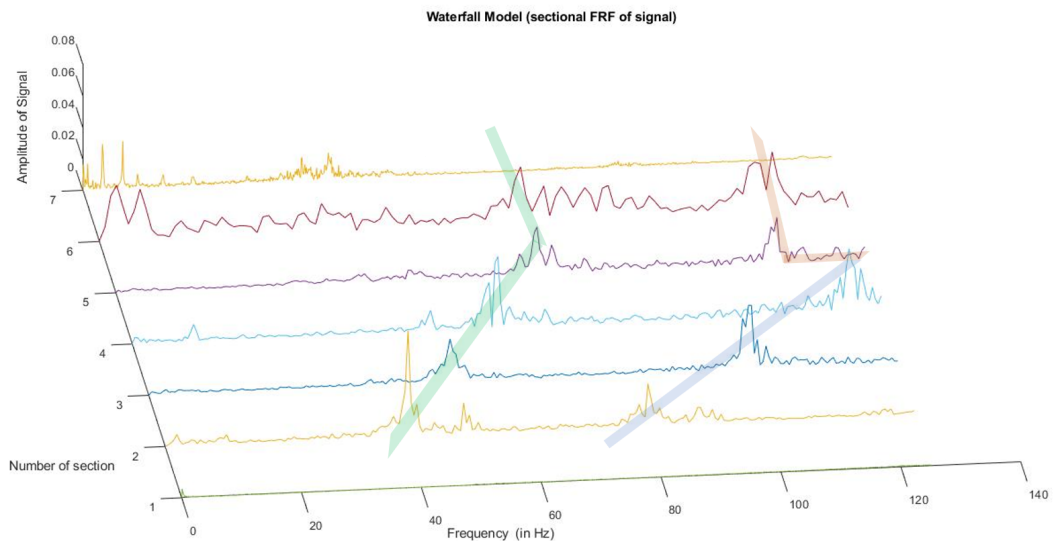


Fig. 6.9. Waterfall model consisting of individual Current signal sections

Fig. 6.9 shows the presence of the disturbance at the frequency half of the tooth passing frequency. As the highest tooth passing from the test (see Fig. 6.6) is 140 Hz which is slightly greater than half of sampling rate of the signal (125 Hz). The system satisfies the Nyquist stability criterion (see equation (3.13)) during the first three signal sections. The latter section of signal consist of tooth passing frequency greater than the Nyquist rate, aliasing can be observed in the signal section (denoted by red line in Fig. 6.9).

Discussion

The power spectrum and waterfall model observes the same disturbances in frequency as the theoretically identified tooth passing frequency of the system (shown in Fig. 6.6). During the latter part of signal we can observe aliasing in the signal as the tooth passing frequency (140 Hz) exceeds the Nyquist sampling rate (125 Hz).

The power spectrum Fig. 6.8 and waterfall model Fig. 6.9 indicates disturbances in the frequency almost half the frequency of the tooth passing frequency increasing in similar steps along with tooth passing frequency. In Fig. 6.9 shows the noises at frequency at half frequency of the tooth passing frequency (denoted by green line starting at 40 Hz). This observed noise at half frequency of the tooth passing frequency can be attributed to a few potential causes:

- The uneven geometry of the tool due to tool-wear.
- The build-up edge which gets deposited in the tool which reduces the cutting ability of the tool.
- The run out error of the cutting tool which induces one teeth of tool to remove more material than another.
- The uneven geometry of the work-piece where the machining operations are carried out.

It can be concluded that the cutting force from the CNC system can only be estimated by filtering the effects of tooth passing frequency from the system. So it is required for the proposed system to compensate the influence of the tooth passing frequency during the machining process.

Chapter 7

Modelling of Disturbance transfer function

The cutting force at the tool-tip is transferred from the feed drive system as a disturbance torque in the servo motor. To accurately estimate the cutting force, it is necessary to design a disturbance observer. This chapter aims to explain the design procedures and methods in modelling the disturbance observer from the hammer test.

7.1 Frequency Response Function (FRF)

During the cutting operation it is not possible to measure the cutting force precisely due to the structural dynamics of the feed drive mechanism. To accurately find the cutting force of the system the frequency range of the disturbance transfer function should be higher than the tooth passing frequency. The disturbance FRF is found out by the hammer test experiment where an impulse force is impacted on the platform where the work piece is mounted. As the measurements from the CNC system and sensorized hammer are of variable sampling rate (250 Hz and 10000 Hz respectively), the signals are re-sampled and manually synchronized to 250 Hz. The FRF of X, Y and Z-axis of the system are shown in Fig. 7.1, Fig. 7.2 and Fig. 7.3.

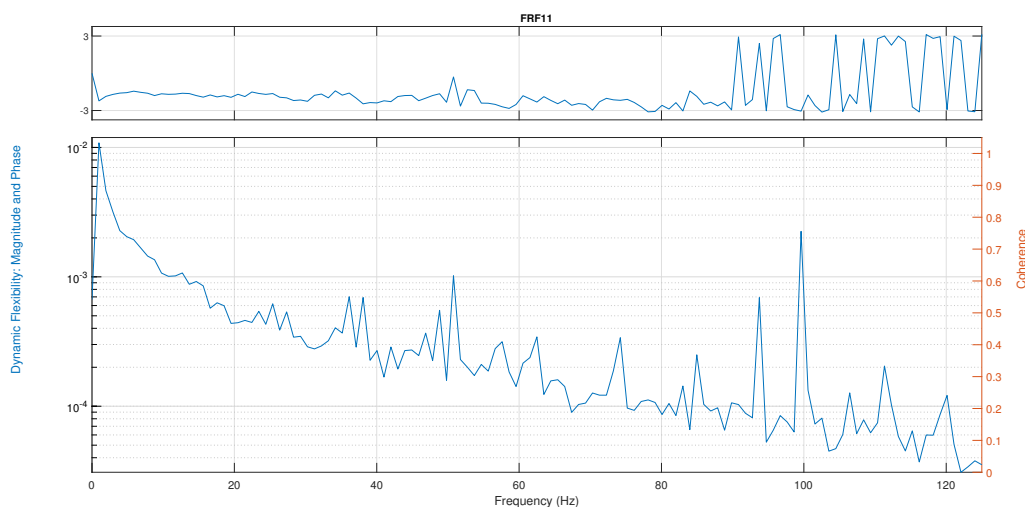


Fig. 7.1. X-axis FRF data from the hammer test

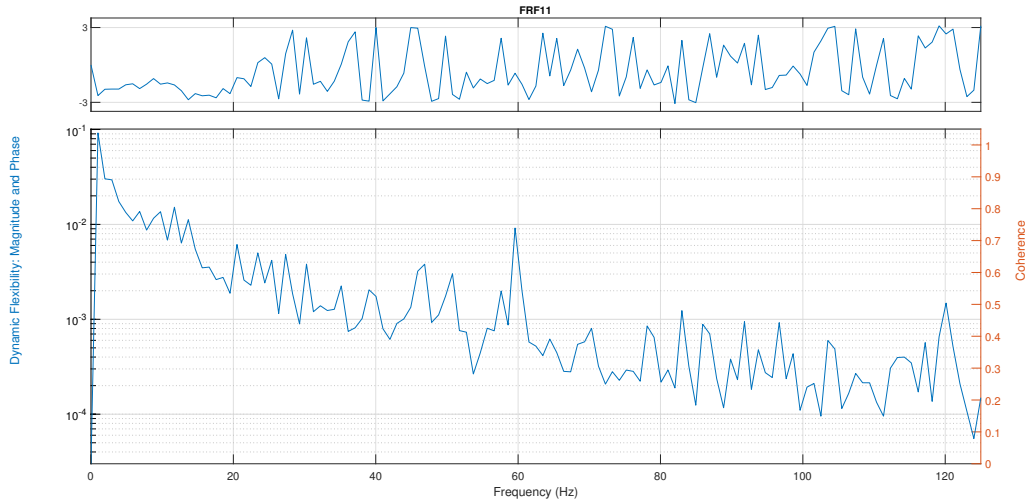


Fig. 7.2. Y-axis FRF data from the hammer test

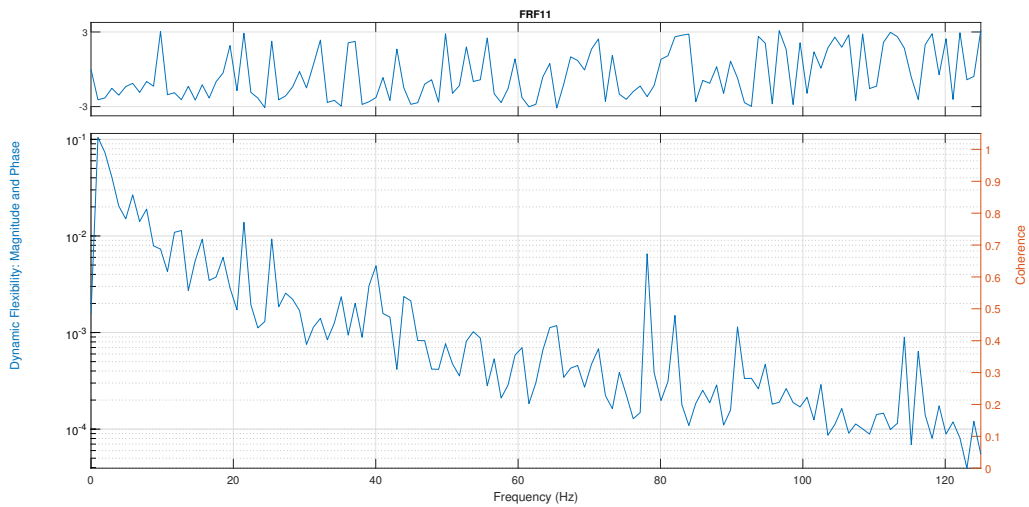


Fig. 7.3. Z-axis FRF data from the hammer test

The disturbance frequency due to structural dynamics of the system is captured by the FRF of the system as shown in figure above. Referring to the Nyquist stability criterion, it is observed that the structural dynamics of the system are only captured until 125 Hz bandwidth (until Nyquist sampling rate). This characteristic FRF of the structural dynamics of the system is used to model the black-box transfer function.

The modelling of the frequency response shown in Fig. 7.1, Fig. 7.2 and Fig. 7.3 are implemented using *Rational Fractional Polynomial* (RFP) curve fitting function in MATLAB. It was observed from the response that the corresponding model can accurately capture the frequencies in the system.

7.2 Transfer Function

Since both sensorised hammer and the machine are of variable sampling rate the data needs to be manually synchronised to 250 Hz. The transfer function for each axis is obtained by manually synchronising the force from the hammer and the disturbance torque from the corresponding servo-controller. By utilizing curve fitting methodology and modal analysis, the transfer function for each feed drive systems are obtained from the frequency response of the system (also see Section 4.3). The transfer function of a system can be denoted by the equation,

$$\Phi_{d(s)} = \frac{\tau_c(s)}{\tau_a(s)} = \sum_k \frac{\alpha_k + \beta_k s}{s^2 + 2\zeta_k \omega_{nk} s + \omega_{nk}^2} \quad (7.1)$$

where α_k , β_k are the residues, ζ_k is the damping, ω_{nk} is the natural frequency of the mode k observed from the RFP curve fitting function, $\tau_c(s)$ is the drive torque of the axis during the hammer impact test and the $\tau_a(s)$ represents the impact torque from the hammer during the impact test [24]. The transfer function is converted into polynomial form and are given by the equation,

$$\Phi_{d(s)} = \frac{\tau_c(s)}{\tau_a(s)} = \frac{b_0 s^n + b_1 s^{n-1} + b_2 s^{n-2} + b_3 s^{n-3} + \dots +}{s^m + a_1 s^{m-1} + a_2 s^{m-2} + \dots +} \quad (7.2)$$

where a_i and b_i represents the transfer function polynomials for each axis of the CNC system [24].

7.3 Dynamic Modelling

The characteristics of the feed-drive dynamics of the five-axis milling machine is captured by performing Hammer-test on the feed-drives (see Section 4.3). The structural modes of the CNC machine are modelled from the corresponding disturbance current provided from the impact of the hammer.

The torque is converted to corresponding force by transmission ratio of the system provided by r_g , given by the equation

$$F_m = r_g \tau_m \quad (7.3)$$

The transmission ratio is used to convert the impact force to corresponding torque measurement. The number of modes, numerator and denominator derived from the transfer function for each axis are shown in Table: 11.1, Table: 11.2 and Table: 11.3 respectively.

The numerator and denominator of the polynomial transfer function is converted to state space form after similarity transformation of the matrices. The mapped state space form is given by

$$\dot{x}(t) = Ax(t) + Bu(t) \quad (7.4)$$

$$y(t) = Cx(t) + Du(t) \quad (7.5)$$

where $x(t)$ is the state vector, $y(t)$ the output vector, A, B, C, D are the state matrices. The state matrices of each axis of the system are derived from the transfer function from the corresponding frequency response data.

7.4 Disturbance Model expansion

The cutting forces at the tool-tip of the CNC machine are influenced by the structural vibrations of the machine. The structural modes of machine are captured by using the disturbance system model. The goal of the expanded disturbance system model is to estimate the harmonic and static disturbances in the feed drive system. These components of the system are utilized by the Kalman filter to rebuild the actual cutting force at the tool-tip of the Five-axis milling machine [24]. The cutting torque can be separated into static and harmonic cutting torque components as shown below,

$$\tau_m = \tau_{static} + \tau_{harmonic} \quad (7.6)$$

The derivative of the static torque component is a constant and is given by static noise ω_{static} .

$$\dot{\tau}_{static} = \omega_{static} \quad (7.7)$$

The harmonic part of the torque component is represented as a function of the tooth passing frequency of the tool. Thus the harmonic component can be represented with a cyclic noise in the Laplace domain as,

$$\frac{\tau_{harmonic}}{w_{AC}} = \frac{s}{s^2 + w_T^2} \quad (7.8)$$

The equation shows the periodic disturbance noise w_{AC} in Laplace domain where the w_T represents the tooth passing frequency of the system [24]. The harmonic disturbance of the cutting torque can be represented in state space equation as,

$$\begin{aligned} \dot{x}_F &= \begin{bmatrix} 0 & -w_T^2 \\ 1 & 0 \end{bmatrix} \begin{bmatrix} \tau_{AC} \\ \dot{\tau}_{AC} \end{bmatrix} + \begin{bmatrix} 1 \\ 0 \end{bmatrix} w_{AC} \\ \tau_{AC} &= [C \quad 0] \begin{bmatrix} \tau_{AC} \\ \dot{\tau}_{AC} \end{bmatrix} + v(t) \end{aligned} \quad (7.9)$$

The disturbance model is expanded by incorporating the harmonic and the static component of the cutting torque into the state space equation. The final disturbance model is represented by the equation,

$$\begin{aligned} \dot{x}_{exp}(t) &= \begin{bmatrix} A & B & BC_F \\ 0 & 0 & 0 \\ 0 & 0 & A_F \end{bmatrix} \begin{Bmatrix} \{x\} \\ \tau_{aDC} \\ \{x_F\} \end{Bmatrix} + \begin{bmatrix} 0 \\ \theta_{DC} \\ \theta_{AC} \end{bmatrix} w(t) \\ \tau_c(t) &= [C \quad 0 \quad 0] \begin{Bmatrix} \{x\} \\ \tau_{aDC} \\ \{x_F\} \end{Bmatrix} + v(t) \end{aligned} \quad (7.10)$$

In the expanded disturbance model shown above, A and B represents the normalized state and input matrix respectively. The A and B matrices are obtained from the transfer-function of the feed drive system. A_F and BC_F represents the state and output matrices of the modelled tooth passing frequency. The expanded disturbance model is used to design the disturbance Kalman filter for reconstructing the cutting forces from the system [24].

7.5 Implementation of Kalman Filter

The dynamic cutting force estimated from the tool-tip of the machine is distorted and consists of the disturbance by the structural dynamics of the machine. The goal of this chapter is to describe the implementation of a Kalman filter based observer to remove the disturbance caused by the structural dynamics of the machine.

7.5.1 Discrete Kalman Filter Design

The approach for Kalman filter is implemented to estimate the discrete cutting forces at tool-tip of the CNC system. The AC component of the torque is modelled as given in the equation (7.9) which describes the periodic disturbance noise produced during the cutting operation.

The Kalman filter takes in the servo-motor current and the disturbance system model to reduce the effect of noises in the cutting force. The expanded disturbance model equation (7.10) is used as one of the input for the Kalman filter design. equation (3.11) and equation (3.12) denotes the equations for implementing Kalman filter. The measured current data from the CNC system is at sampling frequency of 250 Hz, so the disturbance model is discretized with the sampling time of 0.004 seconds. The block diagram consisting of the system variables is shown in Fig. 7.4.

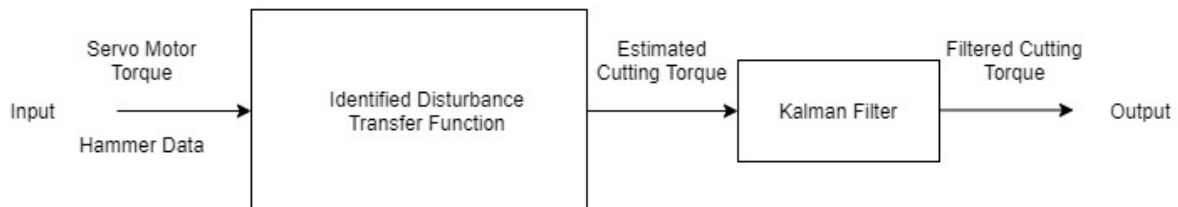


Fig. 7.4. Block diagram of Kalman filter implementation

The accuracy of the implemented Kalman filter is determined by comparing the uncompensated and Kalman filter compensated cutting torque. The comparison of the actual cutting torque before and after applying Kalman filter of an Air cutting section is shown in the Fig. 7.5.

It can be observed from Fig. 7.5 that the Kalman filter reduces the disturbances in the system. To have an accurate estimate of the cutting torque, the Kalman filter is tuned to reduce the noises. Initial condition for the Q and R values are set to zeros and during the Kalman estimation the filter gets updated with the measurement data.

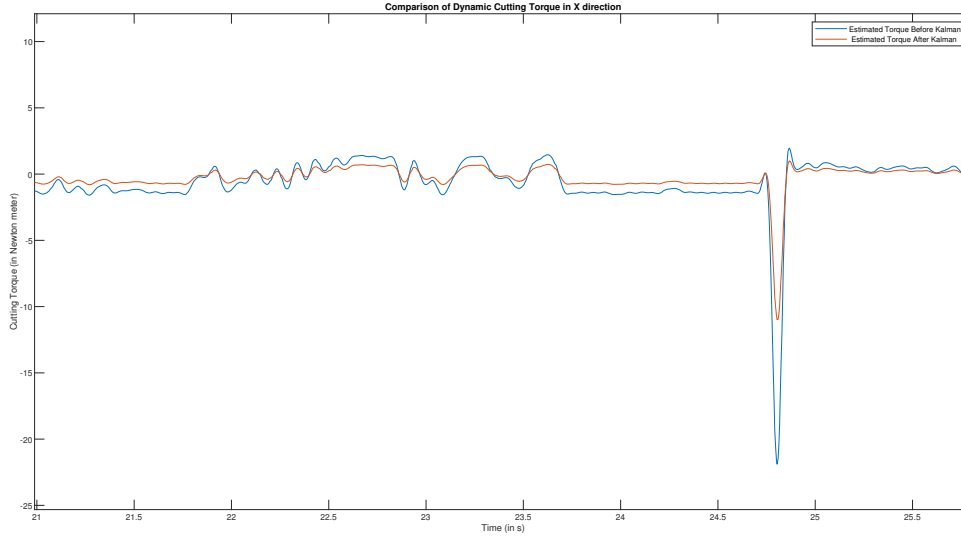


Fig. 7.5. Comparison of Dynamic Air Cutting Torque of a section in X direction

7.5.2 Discussion

The Kalman filter works as a disturbance observer for the estimation of the cutting forces. The input to the Kalman are the torque measurements after eliminating the influence of inertia, friction and the machines dynamics of the system. The aim of the Kalman filter is to reduce the disturbances that are captured in the measured servo-torque signal due to the tooth passing frequency. The total cutting torque of an Air cutting experiment is zero but it can be observed from the Fig. 7.5 that the estimated cutting torque of the air cutting section consists of noises. This disturbance in estimation can be accounted due to the inaccuracy in eliminating the inertia and friction parameters of the system.

A discrete Kalman filter approach is implemented in the scope of thesis work. The implementation of the discrete Kalman filter is preferred due to:

- The variable sampling rate of the servo-motor which varies from 200Hz to 250 Hz.
- Missing data points in the CNC data acquisition system during machining operation.
- The sampling rate of the machine is very low (200 Hz) compared to the sampling rate of dynamometer (20000 Hz).
- The discrete Kalman filter approach is less complex compared to the continuous filter method.

7.5.3 Filter Tuning

The system and the noise co-variance matrices are presumed as zero white Gaussian noises with co-variance matrices. The measurement co-variance matrix (R) and the system noise co-variance matrix (Q) for each axis is required to tune the Kalman filter.

The matrices Q and R are tuned to compensate the error of the system. The changing Q matrix tunes the noise in the system and R matrix tunes to the noise in the measurement. The R values is obtained from the RMS of the torque variation values while

conducting the air cutting experiment. The values of the Q matrix is determined by trial and error combination. Initially to begin, the values of the Q matrix are set to zeroes and ones. Observing the cutting force from the Kalman filter the values are changed in-accordance to the estimation output. Finally a better estimation can be achieved by tuning the Q , R matrices and assigning the weights to both noise matrices.

7.6 Conversion of Torque to Cutting Force

The linear feed drive axis uses ball screw mechanism in between the motor and the table. To convert the estimated torque at the motor to force at the tool we use the equation given by,

$$F_a = \tau_c \frac{\eta}{r_g} \quad (7.11)$$

$$r_g = \frac{P}{2\pi}$$

where F_a is the estimated force, τ_c is the estimated torque after Kalman filtering η is the efficiency, r_g is the transmission ratio and P is the pitch of linear axis. [24].

Chapter 8

Validation Tests

The cutting force estimated from Kalman filter is validated by comparing against the force from the dynamometer measurement. The goal of this chapter is to provide an outline of the validation setup and the design methodology for verifying the estimated cutting force.

8.1 Experimental Setup for validation

The validation of the suggested black-box model is determined by comparing the estimated force measurement with the force measurements from the dynamometer. The validation tests are performed using only the linear axes of the machine tool. The rotary axes are avoided due to direct drive mechanism in rotary axis. The experimental setup for the validation tests are shown in Fig. 8.1.

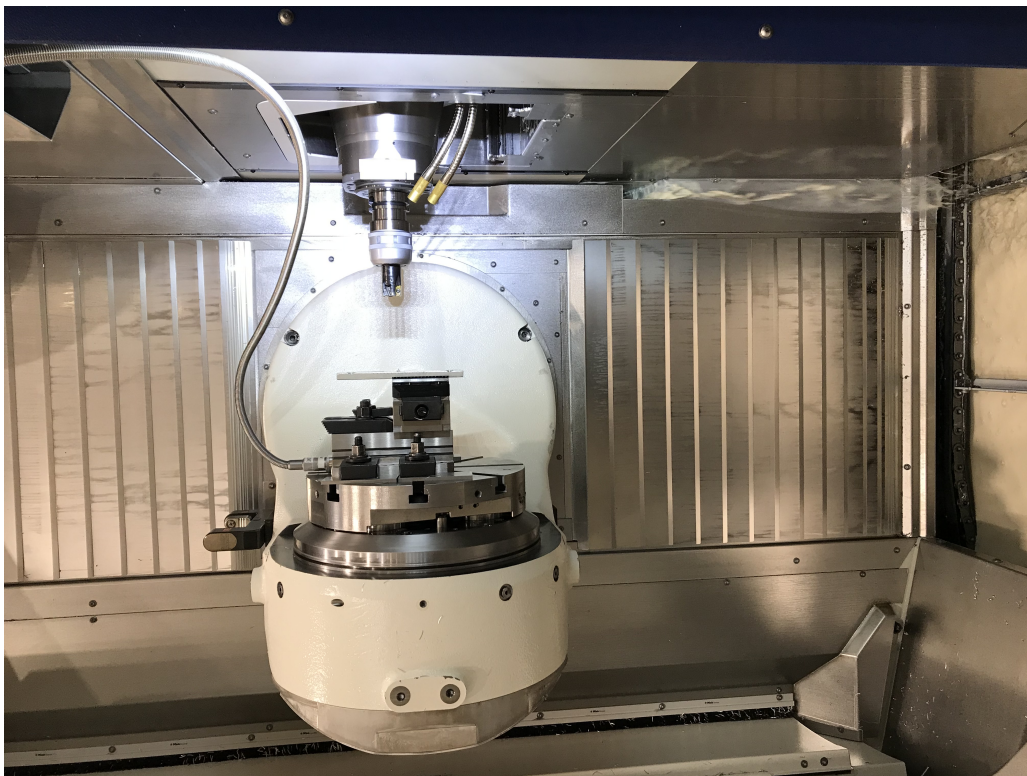


Fig. 8.1. Experimental Setup for validation of Cutting Force

The experimental setup consists of a Kistler dynamometer attached to the table of the CNC machine, work-piece and the two teeth milling tool. The cutting experiments are carried out on five-axis CNC machine and is differentiated based on Air-cutting (without a work-piece) and Cutting experiment (with work-piece) with two teeth tool.

The piezo-electric dynamometer captures the cutting force produced at the tool-tip during the cutting operation. The CNC machine and the dynamometer are synchronised to an external data acquisition module to collect data during the same time interval. The collected data from the external data acquisition system are used to validate the proposed system.

The experiment signals are collected from the CNC machine, dynamometer and are saved in *Labview* software as *TDMS* (Technical Data Management Streaming) file. The files are then manually converted to *Microsoft Excel* for analysing and validating proposed model in MATLAB.

8.2 Validation Tests

Validation tests are performed to verify that the suggested system model accurately predicts the cutting force from servo-torque measurements. Validation data for the Kalman estimator consist of the measurements from the servo-controller as well as the corresponding force measurements from the dynamometer. The servo-drive and dynamometer measurements are extracted with the help of a National Instruments data acquisition system. This external acquisition system synchronises both dynamometer data and the CNC measured data to the same interval of time.

The validation tests are performed to check the accuracy of the estimated system model. The data collected while performing air cutting experiment and real cutting tests on the Five-axis milling machine and is shown in Fig. 8.3 and Fig. 8.4 respectively.

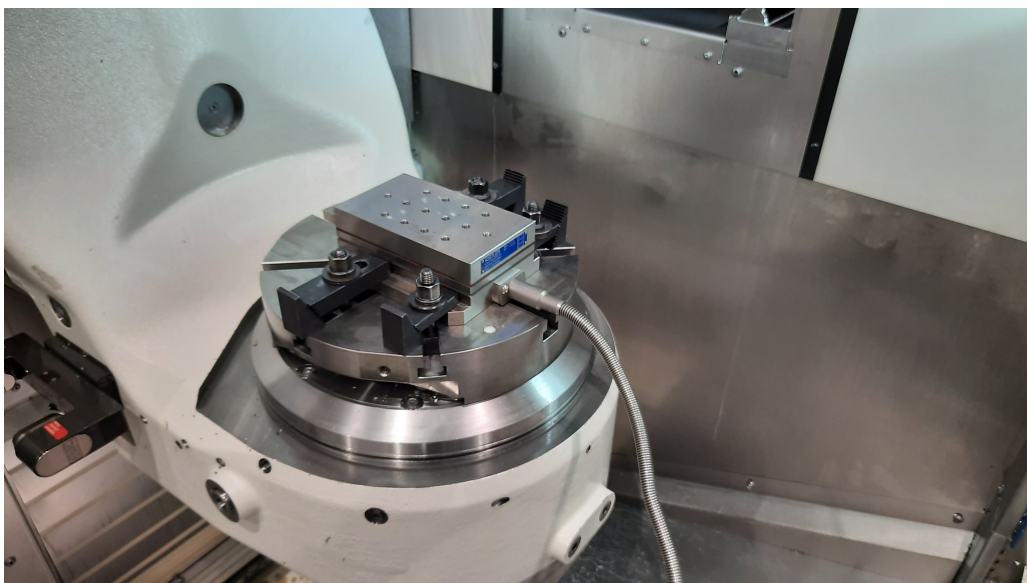


Fig. 8.2. Kistler dynamometer attached to table

Fig. 8.2 shows the experimental setup of how the dynamometer is attached to the CNC table. After processing the data, the force estimated from the validation test are compared with the dynamometer cutting force measurement. The accuracy and errors of the system are calculated from the measurement.

The validation tests are divided on the basis of presence of work-piece as Air cutting tests and Cutting tests.

8.2.1 Air cutting Experiment

The air cutting experiment involves the machining which is performed without the presence of work piece while measuring the corresponding servo signal from the CNC machine. The cutting force at tool-tip at any instant of time during an air cutting experiment is zero. This principle of the air cutting experiment is used to determine and verify the estimated cutting force at tool tip. Fig. 8.3 shows the servomotor signals data during an air cutting experiment.

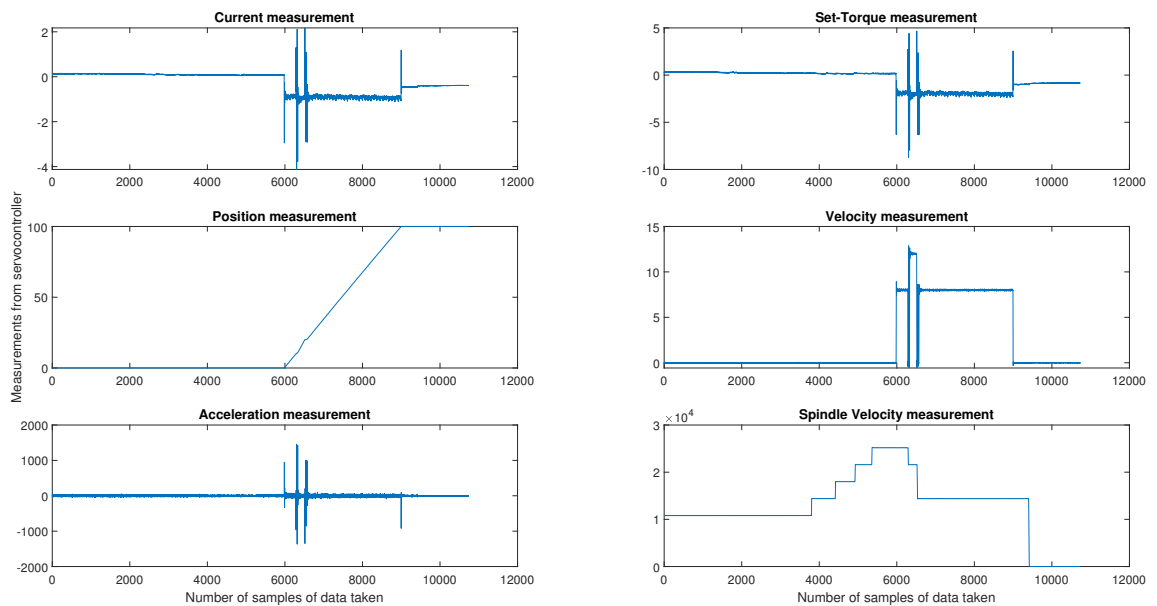


Fig. 8.3. Air cutting measurements from the servo-controller for X-axis

The estimated force from the proposed system is compared with the force measurement from the dynamometer to determine the accuracy and the percentage error in the proposed model.

8.2.2 Cutting Experiment

The cutting experiment consists of the series of machining tests which are performed on the work piece by the tool attached to the machine. The machining tests are performed at

a varying low speed velocity to observe the influence of varying speed over tooth passing frequency. Finally, the estimated dynamic force calculated at the tool-tip during the cutting experiment is verified by comparing against the dynamometer force measurement.

The cutting experiment is performed at a low spindle speed to reduce the effects of aliasing observed in the measured servo-drive signals. Fig. 8.4 shows the servomotor signals for X-axis data from the cutting experiment performed on the CNC machine. The figure (Fig. 8.4) also shows the influence of varying tooth passing frequency with respect to the varying spindle speed of the five axis machining.

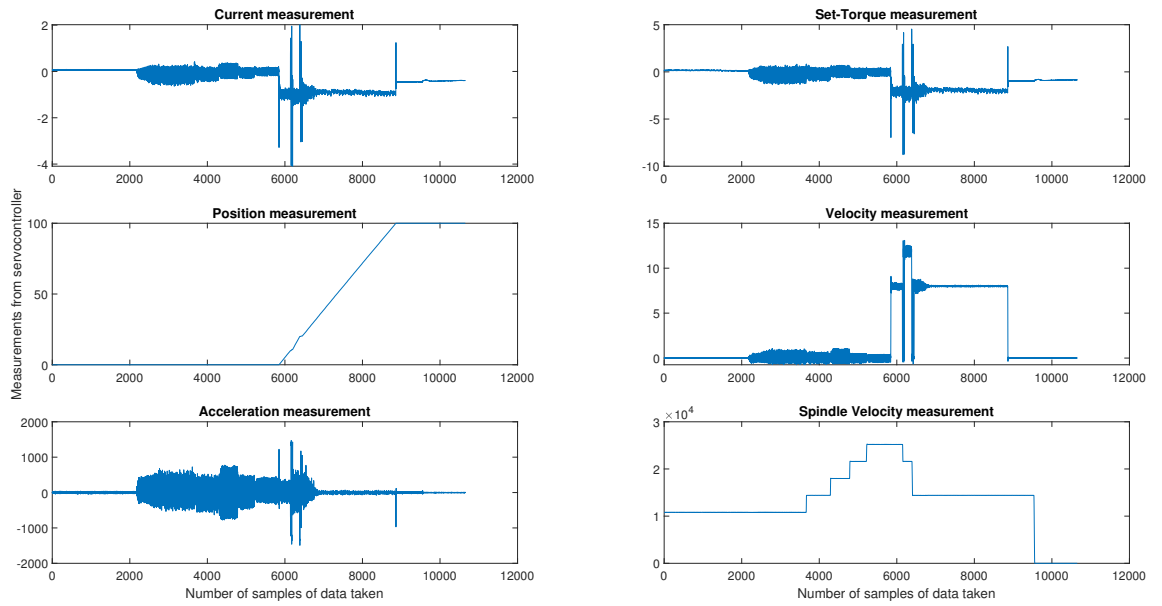


Fig. 8.4. X-axis measurements of servo-controller for the Cutting experiment

The force exerted by the tool-tip is identified by the system model and compared with the force measurements from the dynamometer. The system is validated and the accuracy, the error percentage in comparison to the dynamometer measured force data is computed.

8.2.3 Dynamometer Measurement Setup

While conducting the experiment the Kistler dynamometer is oriented in different direction from the CNC system (as shown in Fig. 8.1). The direction of the Y-axis of dynamometer aligns with X-axis of machine, X-axis of dynamometer aligns with the Y-axis of machine and Z-axis of both machine and dynamometer aligns in the same direction. The dynamometer setup for measuring force can be seen in Fig. 8.2 and is oriented 90 degrees during the machining operation (see Fig. 8.1).

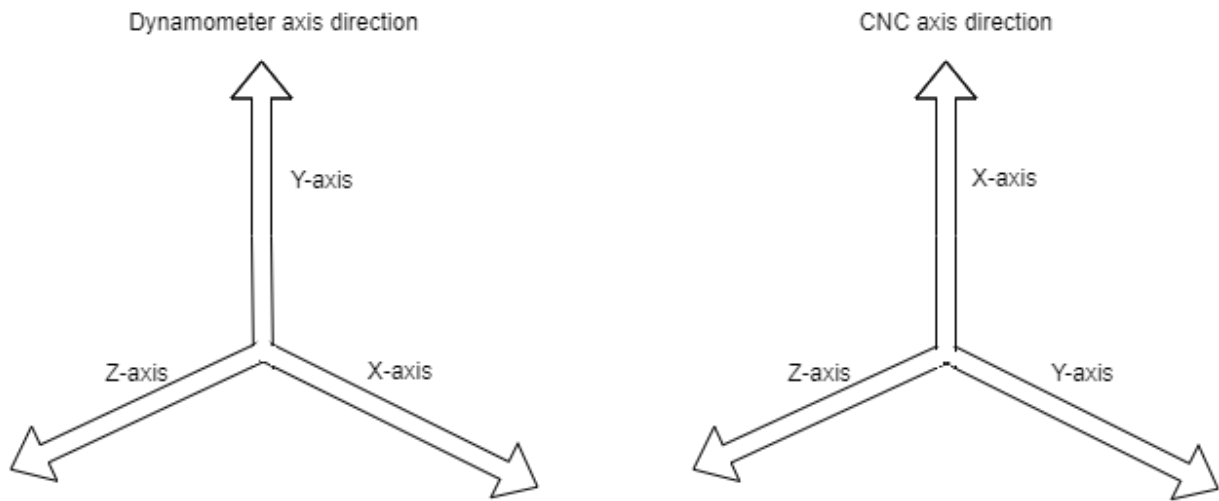


Fig. 8.5. Dynamometer Axis direction in comparison to CNC Axis

Fig. 8.5 represents the axis of the dynamometer with respect to the axis of the CNC machine. The Y-axis measurement of the dynamometer yields the output of X-axis of the CNC system, the X-axis measurement of the dynamometer yields the Y-axis of the CNC system and Z-axis remains same for dynamometer and CNC system.

Chapter 9

Results and Discussion

This chapter focuses on the cutting force measurements obtained from the verification tests and a discussion on how the observed cutting force measurements are justified. The chapter also briefly discusses about the accuracy and the reliability of the estimated system in comparison to the Dynamometer.

9.1 Air cutting Test

Air-cutting experiments (see Section 9.2.1) are performed on the five-axis system to analyse and verify the estimated black box system model. The principle behind the estimation depends on the fact that the total force at any moment during air cutting test is zero. The output force from the different axes of the dynamometer is provided in the Fig. 9.1.

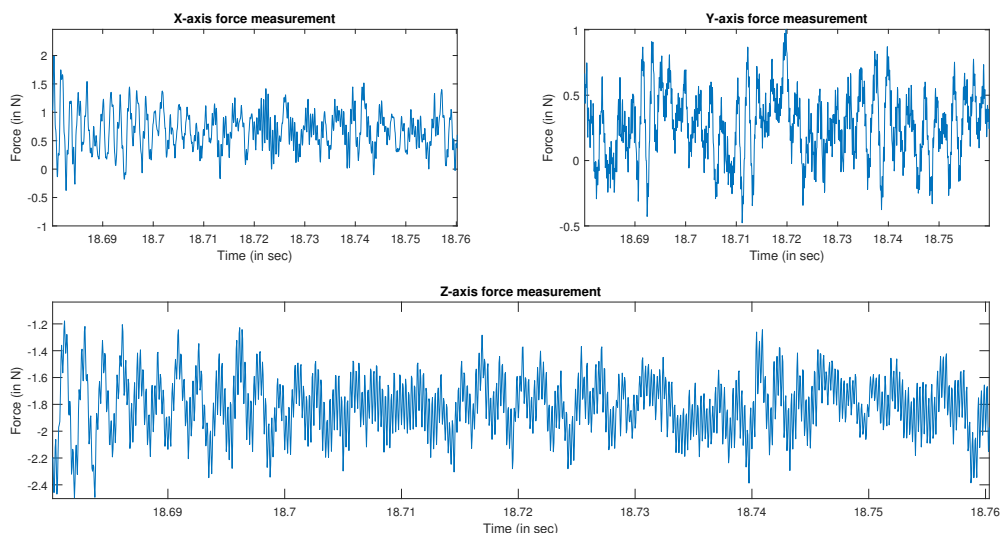


Fig. 9.1. Dynamometer force of a section for each axis during Air cutting test

The force measured from the dynamometer is used as the reference (ground-truth) to compare the estimated output from the Kalman estimated system model. The reliability of the dynamometer is analysed by the FRF of the measured dynamometer force. The accuracy of the estimated model is measured by comparing the output with the corresponding force measurement from the dynamometer.

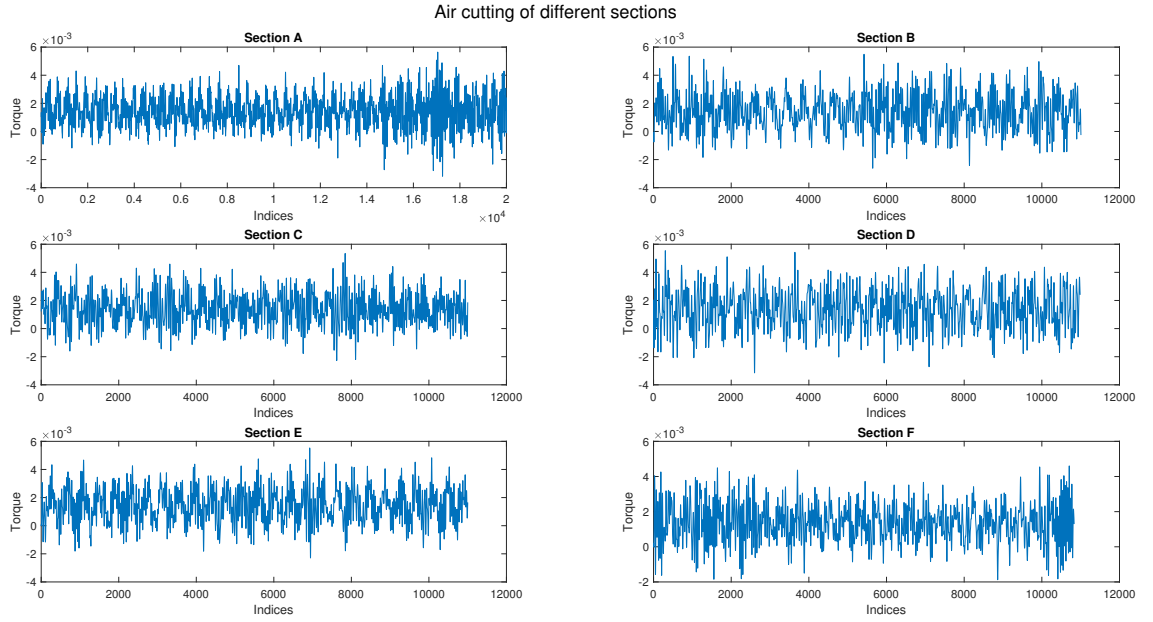


Fig. 9.2. X-axis sections of servo-torque during Air-cutting experiment

The servo-drive torque measurement is divided into different sections to make the analysis easier. Fig. 9.2 shows the subdivision of servo-drive torque corresponding to different tooth passing frequencies. The validation of the estimated system model is performed by analysing sectional force to the corresponding dynamometer force.

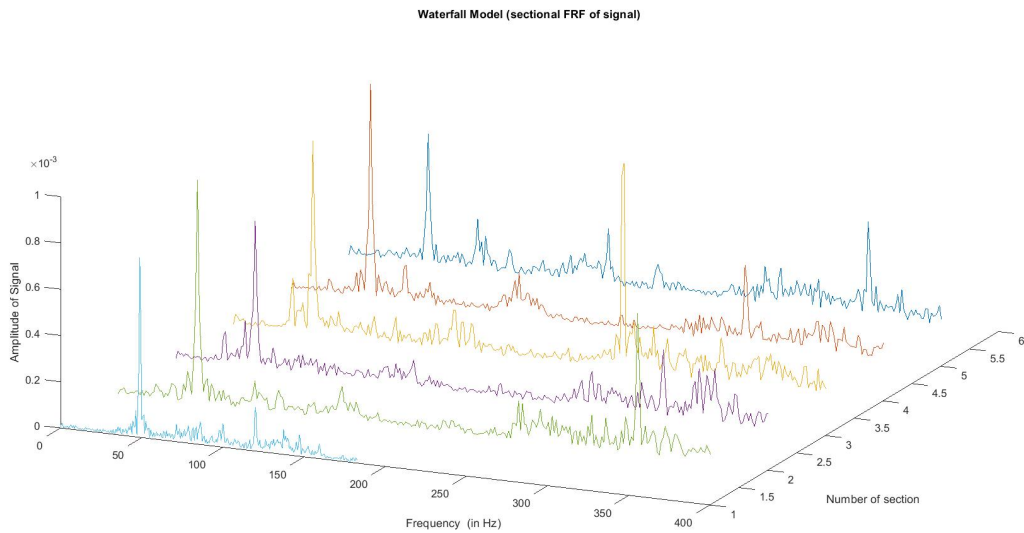


Fig. 9.3. Waterfall model of X-axis sections of Dynamometer measurement

Fig. 9.3 shows the waterfall model created from the sections (varying tooth passing frequency) of the measured dynamometer signal. The waterfall graph shows each section of signal having constant frequency disturbance closer to 40 Hz. This constant disturbance observed in FRF of the waterfall graph is caused due to the structural dynamics of the CNC machine. The waterfall graph shows no disturbance of frequencies until 250 Hz

which is expected during an air cutting experiment. The FRF analysis in waterfall graph provides information regarding the accuracy and trustability of the dynamometer system.

To analyse the force transformation of the system, the transmission ratio and torque constant are determined from the static load test. The estimated force from the dynamometer system is compared with the force from the model as shown in Fig. 9.4 and Fig. 9.5.

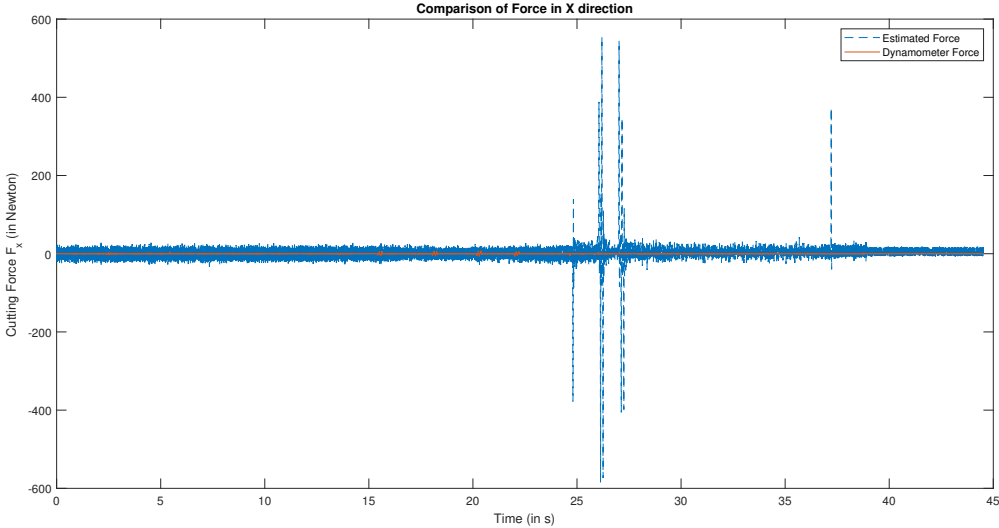


Fig. 9.4. Comparison between Estimated Force and Dynamometer force

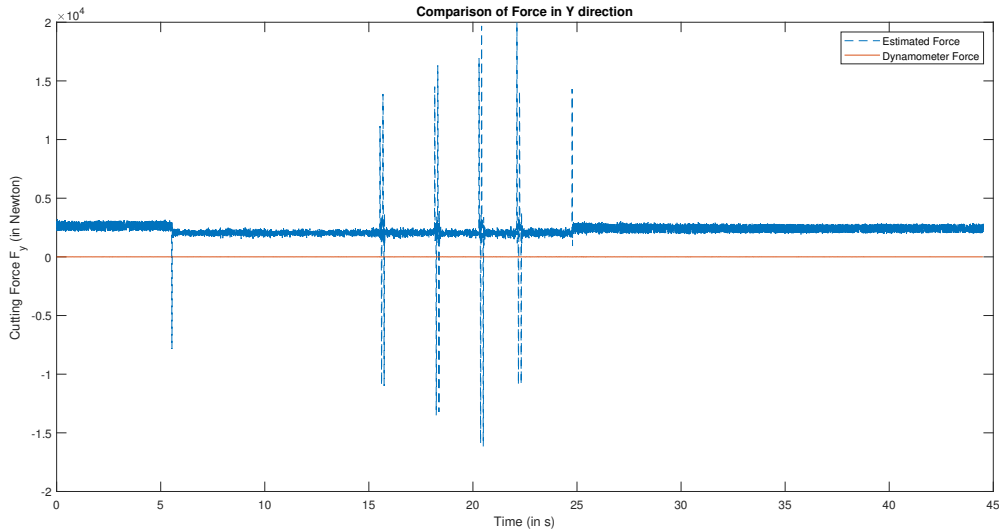


Fig. 9.5. Comparison between Estimated Force and Dynamometer force

To analyse the forces more accurately, a small section of the forces are considered as shown in the Fig. 9.6 and Fig. 9.7.

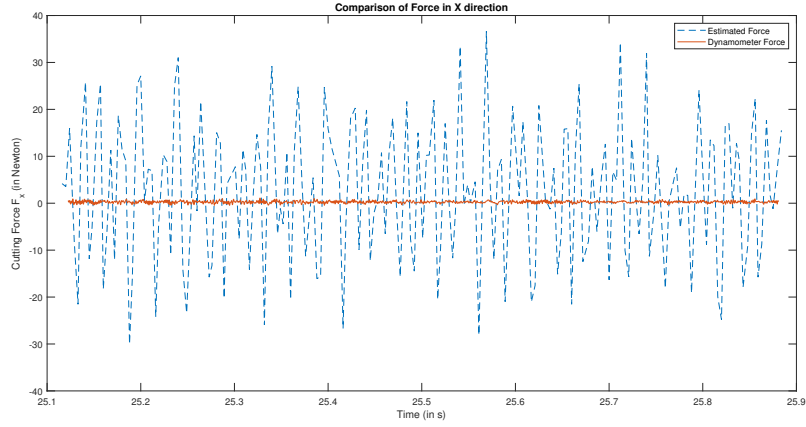


Fig. 9.6. Comparison between Estimated Force and Dynamometer force

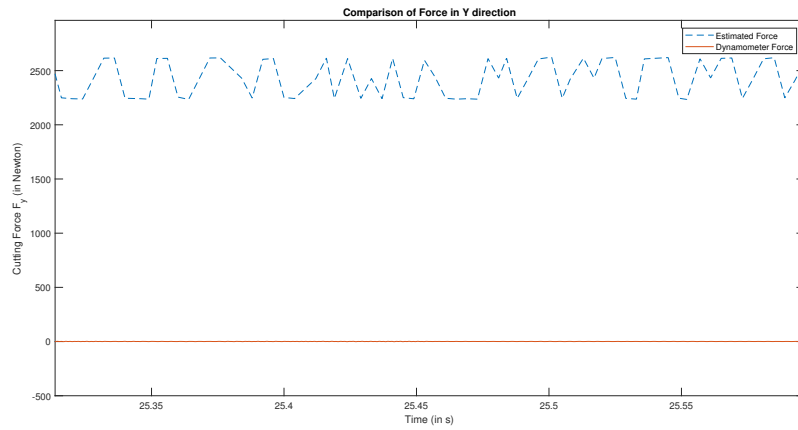


Fig. 9.7. Comparison between Estimated Force and Dynamometer force

The similarity between the measurements are determined by comparing both dynamometer and estimated the cutting forces in the selected signal section. A static cutting force is observed in the proposed system in Y direction. The static force can be attributed to the rotary axes carried by Y axis. The high cutting force from the CNC model in Y direction around 2300 N is observed also due to the variable offset at the beginning of the torque signal produced from the servo-drive.

9.1.1 Discussion

Fig. 9.4 and Fig. 9.5 show the comparison between the estimated force from CNC and the measured cutting force from the dynamometer. The figure shows a pseudo-force at the start and the end of the estimated cutting force from the proposed model. This distortion is caused due to the inaccuracy in modelling the friction parameters of the CNC system as the proposed friction model doesn't capture the Stribeck friction of the CNC system (see Section 5.1).

The cutting force at any moment of time during an air cutting experiment is expected to be zero, but the measurement is distinct from the expected value in Y direction (see

Fig 9.5). A high cutting force is observed at the estimation from the proposed system. This observable high force is caused due to the Y axis drive carrying A and C axis drives of the CNC system and also due to static offset in the CNC measurement.

To provide a clear analysis of the static offset force, the measurements from different cutting experiments are taken into consideration. From the comparison of servo-torque measurement, it is observed that the offset varies during each experiment and this causes a static pseudo force in the estimated value of the proposed model.

The air-cutting experiment concludes the result that the static force in Y-axis of the proposed model can be determined accurately only by calculating the offset force of the servo-torque measurement of the system.

9.2 Cutting Test

The verification of the proposed system model is determined by performing real cutting test (see Section 9.2.2) on the work-piece. The cutting experiment is performed in XY direction to validate the proposed model in linear axes. During the cutting experiment, the corresponding dynamometer and servo-drive measurements are collected and analysed with the help of an external data acquisition system.

The cutting test is carried out with with a two teeth tool with low spindle speed to reduce the inaccuracies due to aliasing (see Section 9.2.2) and the friction model (see Section 5.1). The work-piece for the two axis cutting test is shown in Fig. 9.8.

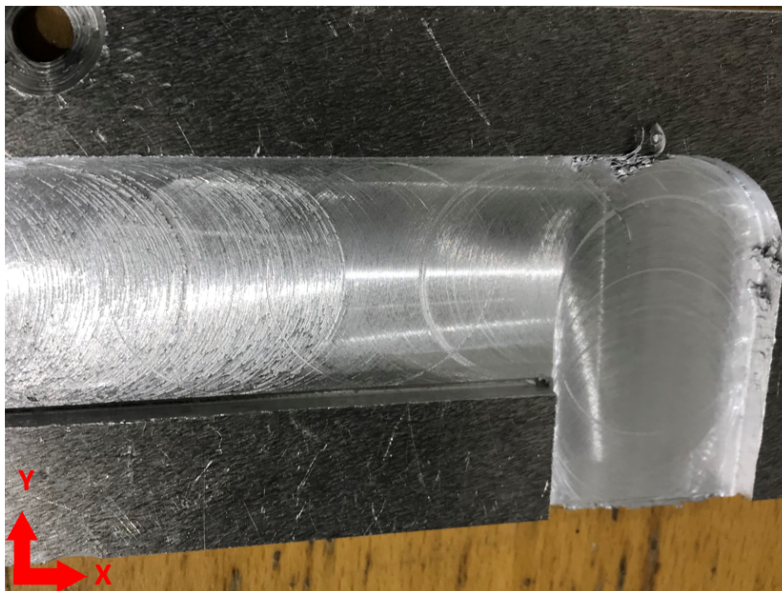


Fig. 9.8. Workpiece after performing two-axis cutting test

The Fig. 9.9 shows the force value measured by the dynamometer in X,Y and Z axis with a sampling rate of 20000 Hz. The measurement from the dynamometer is used to determine the accuracy of the proposed system model.

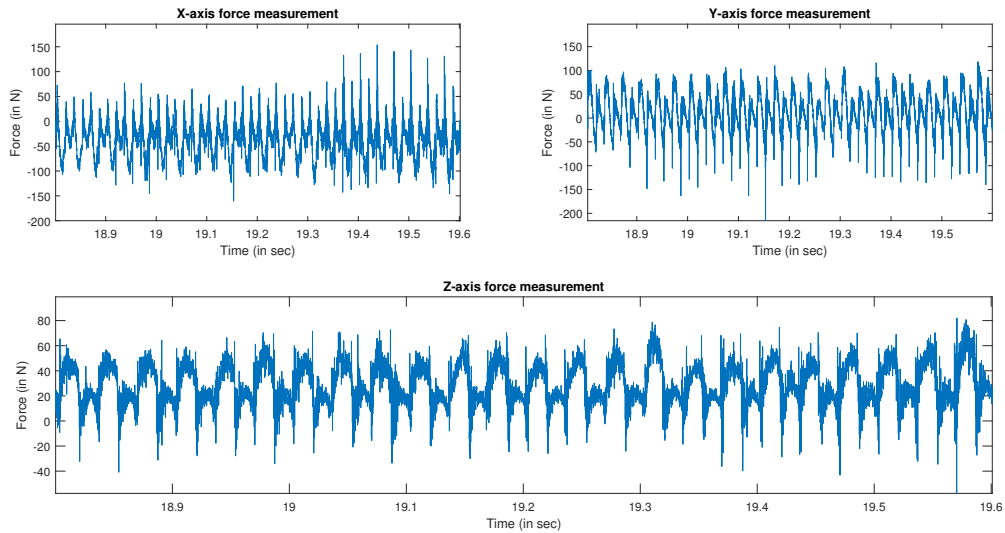


Fig. 9.9. Measured Dynamometer Force for a particular cutting test

The tooth passing frequency is observed in each sections increasing from 50 Hz to 100 Hz. To analyse the reliability of the dynamometer force, the FRF of the dynamometer measurement is plotted as a waterfall model. Fig. 9.10 shows the waterfall model of the dynamometer.

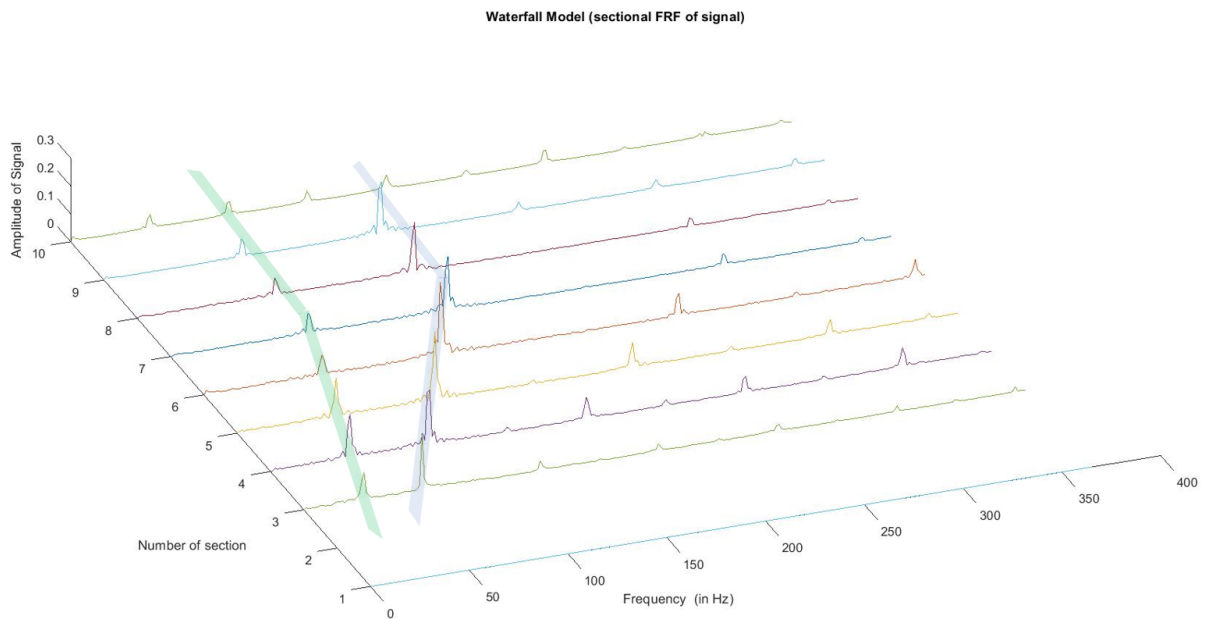


Fig. 9.10. Waterfall model obtained by analysing FRF of different sections

A disturbance is observed at the tooth passing frequency and an additional unexpected frequency observed at almost half of the tooth passing frequency.

The sampling rate of the dynamometer system is very high (20000 Hz) compared to servo-drive measurement system (250 Hz). To analyze the torque measurements clearly, the torque measurements are divided into various sections based on difference in the

tooth passing frequency. Each section of the system is analysed distinctly to determine the accuracy of the proposed model. To analyse the force transformation of the system, the transmission ratio is determined from the static load test.

The division of the servo-torque sections based on tooth passing frequency is shown in Fig. 9.11.

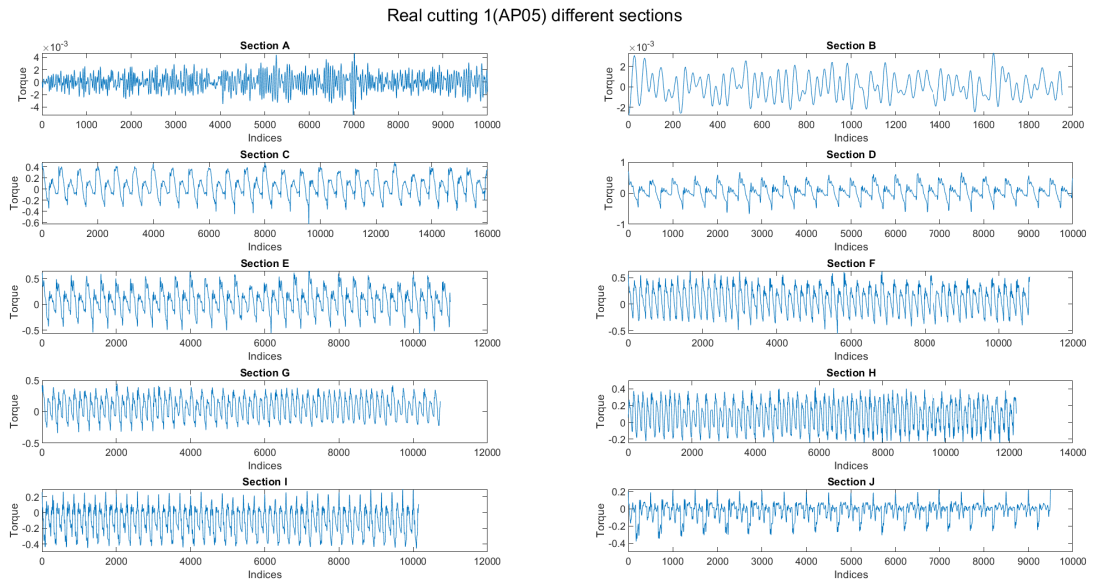


Fig. 9.11. Cutting torque sections of X-axis with respect to tooth passing frequency

To determine the accuracy and reliability of the cutting force estimated, the cutting force from proposed model is compared with the dynamometer measured force. To make the comparison easier a particular section of the servo-torque is considered.

The comparison between the experimentally measured and estimated forces for X and Y direction are shown in Fig. 9.12 and Fig. 9.13. The difference between the sampling frequency of the estimated and measured system can be clearly observed in Fig. 9.12. This can be avoided by filtering the dynamometer force to compare the accuracy in force estimation.

It is also observed that the static force component of Y axis is very high than the static component of the dynamometer force. This can be attributed to the offset present in the start of measurements from the CNC system.

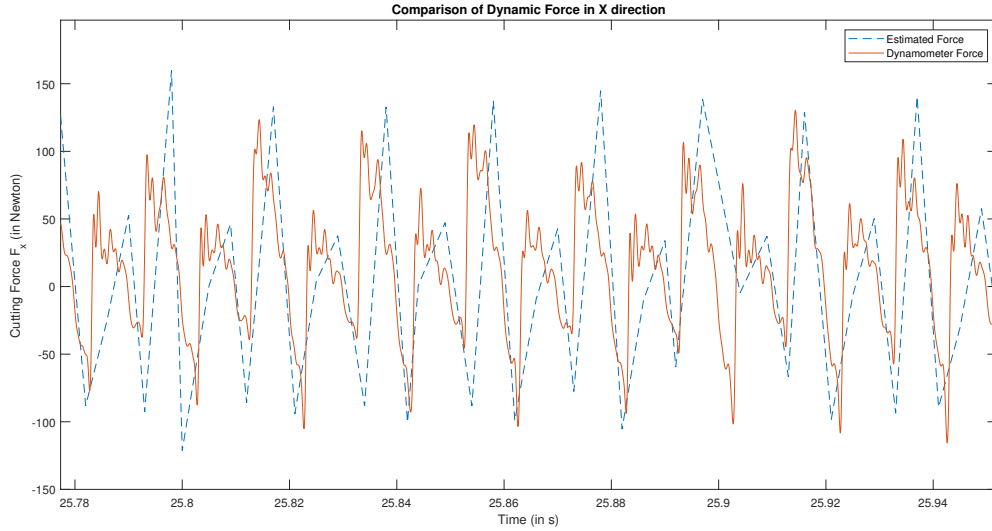


Fig. 9.12. Comparison between experimentally measured and estimated force

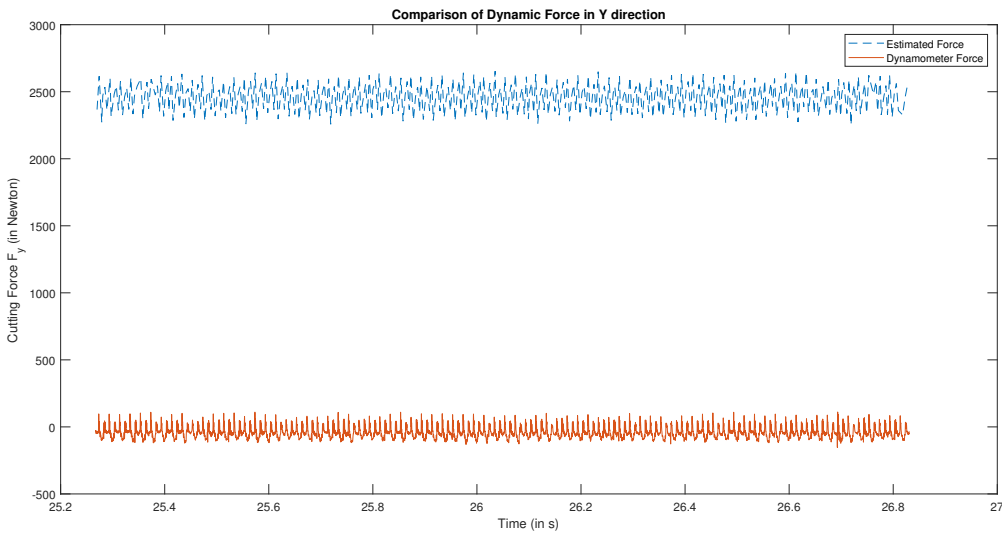


Fig. 9.13. Comparison between experimentally measured and estimated force

The static component of force in the CNC system cannot be accurately estimated in Y axis due to the presence of offset in the system (See Section 10.1). This offset in Y axis of the proposed system may be attributed to the cause that Y axis carries A and B axis of the CNC machine.

To analyse the accuracy of the estimated system the dynamic and the static components of force is measured against the corresponding dynamometer components of the force.

9.2.1 Static Force Comparison

The static component of the force is captured by removing the dynamic force components through a lowpass filter. The static forces in X and Y direction are shown in the Fig.

9.14 and Fig. 9.15.

We can observe from the figures that there are high frequency components present in the static force measurement even after filtering the dynamic components of the force. The static force in Y direction (shown in Fig. 9.15) detects an offset in force. This is due to the presence of variable offset in the start and end of the measurement.

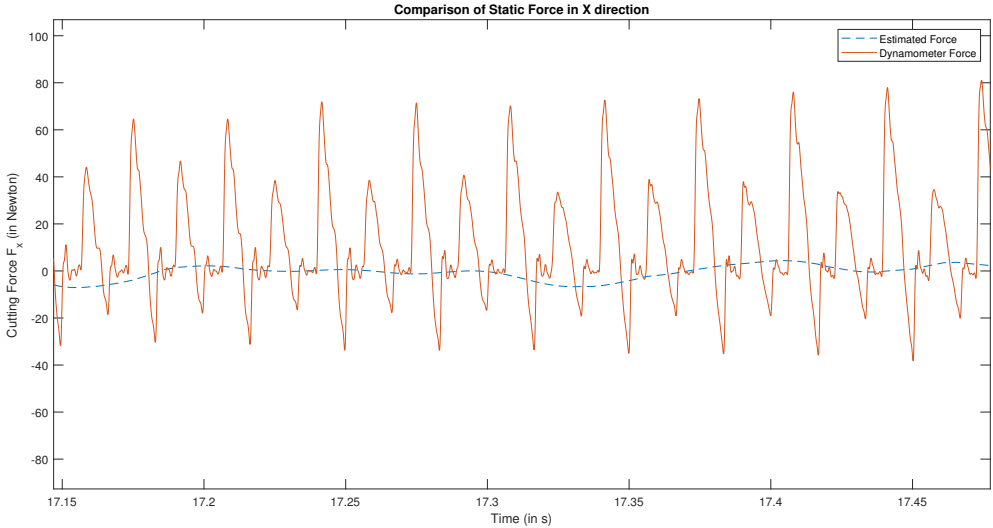


Fig. 9.14. Comparison between experimentally measured and estimated static force

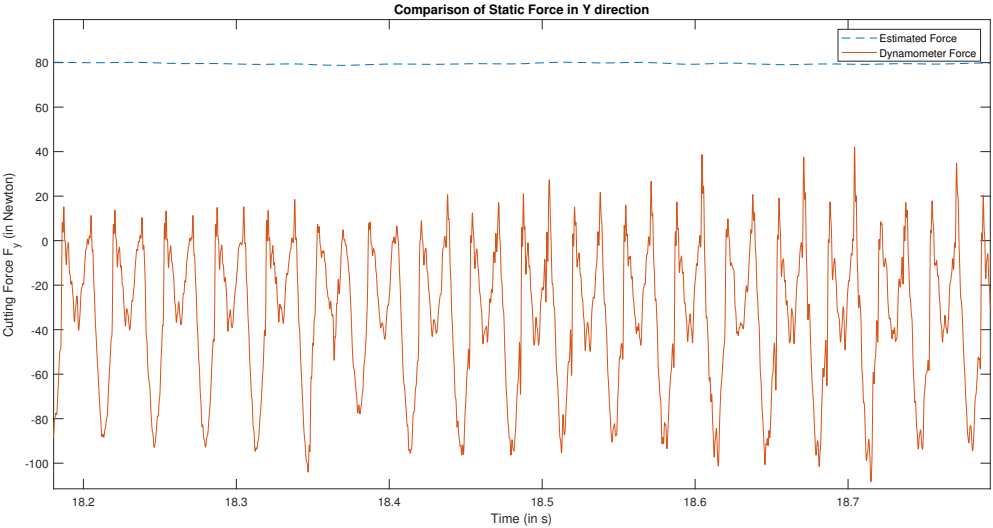


Fig. 9.15. Comparison between experimentally measured and estimated static force

By repeating the comparison of static force components, it can be observed the static forces are influenced by drifts in the system, which is caused by the CNC system. The small drift over time in the static force of CNC system can be observed in Fig. 9.16

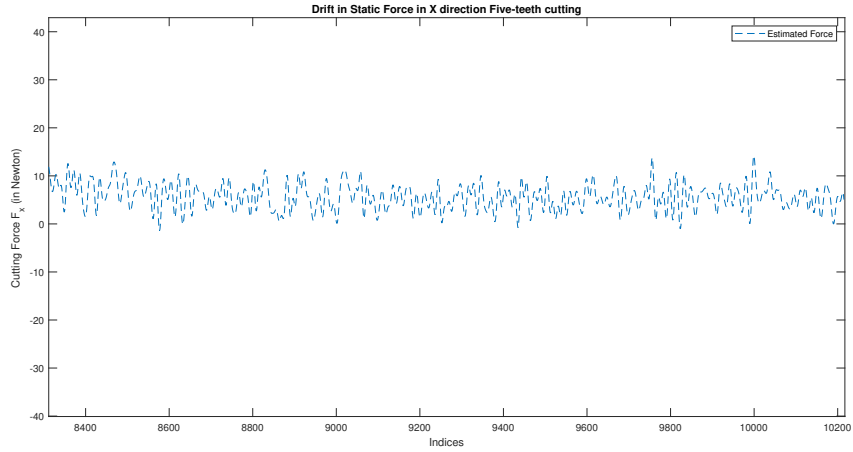


Fig. 9.16. Drift observed in estimated static force in Five teethed machining

Due to the presence of offsets, drifts in measurement and noises in the static component of the force measured from dynamometer and the system, the static force during machining cannot be accurately estimated. This concludes that the static components of the force measurement cannot be measured by the proposed system.

The comparison between dynamic force components are performed to check the accuracy of the system.

9.2.2 Dynamic Force Comparison

As the static component of the estimated force is affected due to the frequency component of the dynamometer system and offset, the dynamic component of the force estimation is only considered. The dynamic component of the force is captured by removing the static force components through a highpass filter.

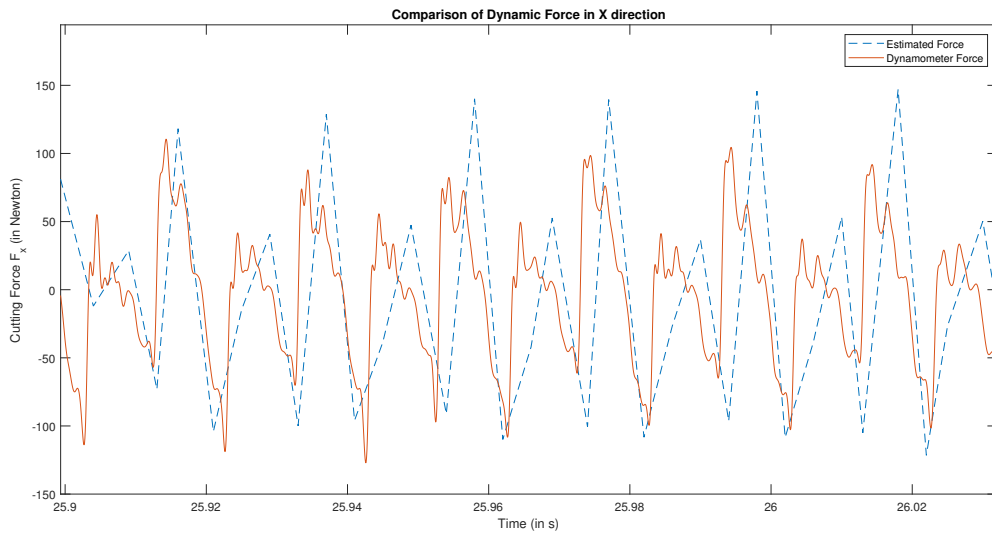


Fig. 9.17. Comparison between experimentally measured and estimated dynamic force

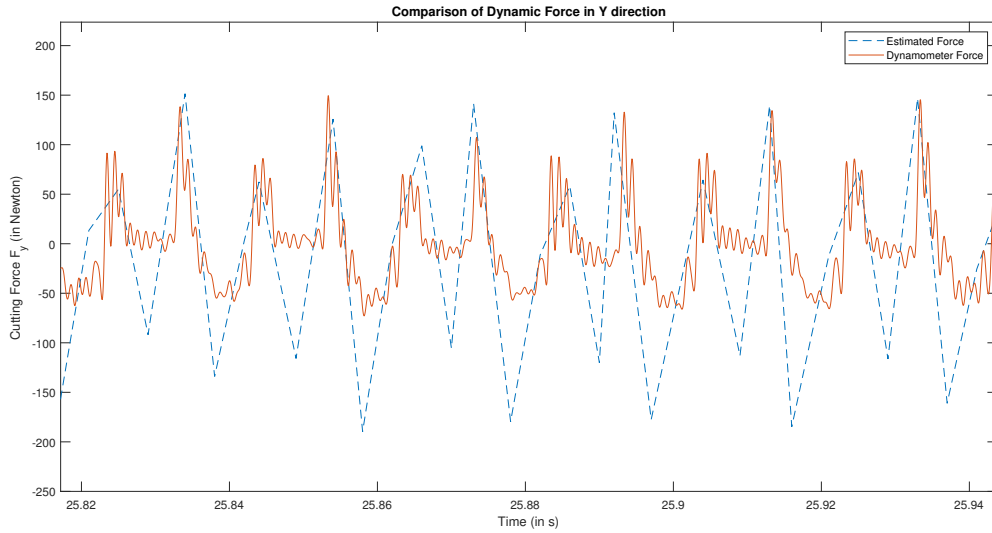


Fig. 9.18. Comparison between experimentally measured and estimated dynamic force

The comparison of dynamic forces in X and Y direction is shown in the Fig. 9.17 and Fig. 9.18. From the figures we can observe that there are high frequency components present in the dynamometer measurement even after the measurement is filtered at 200 Hz. To accurately compare the force measurements a moving average filter is implemented.

Using a Moving Average filter

To compare the estimated and measured forces accurately a 30-point moving average filter is implemented on the dynamometer force along with the low pass filter.

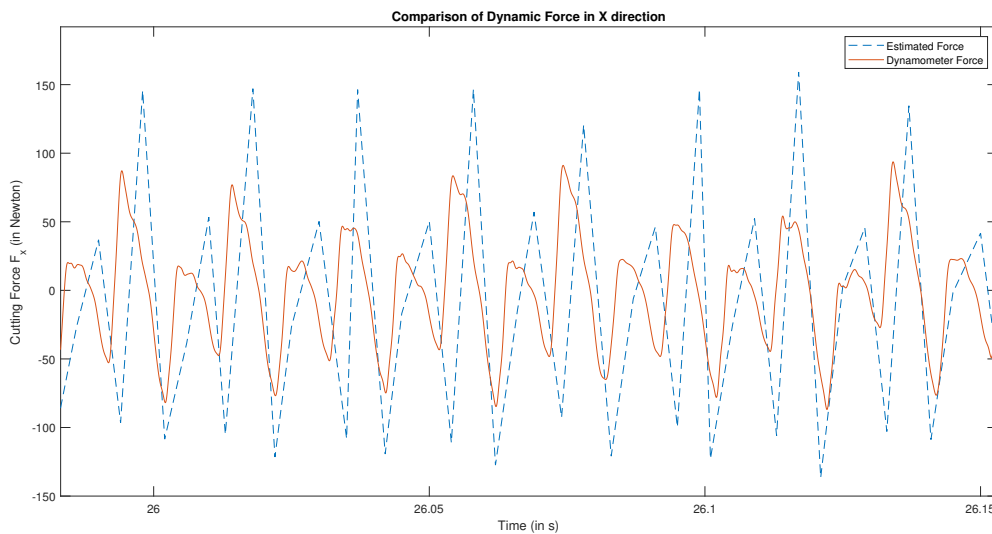


Fig. 9.19. Comparison between experimentally measured and estimated dynamic force

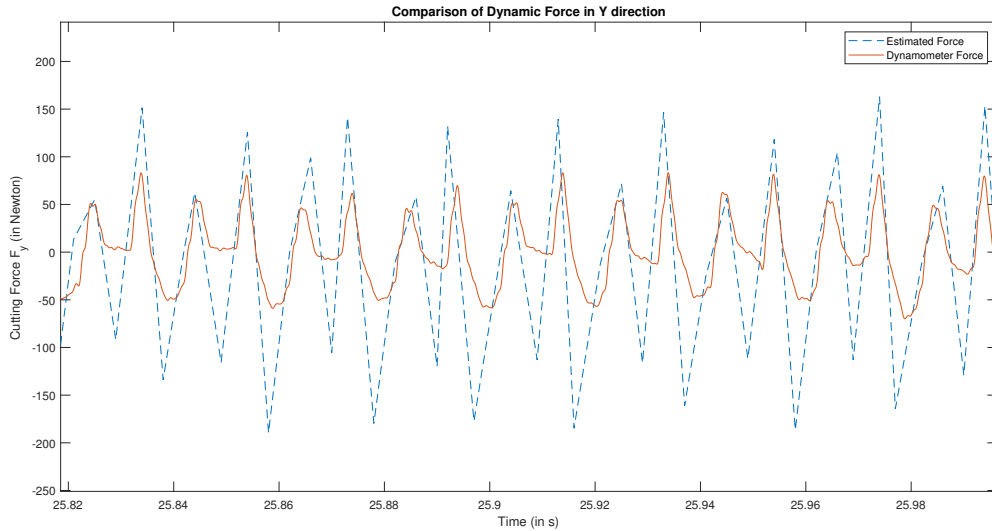


Fig. 9.20. Comparison between experimentally measured and estimated dynamic force

As seen from the Fig. 9.19 and Fig. 9.20, it is observed that the estimated forces are in agreement with the measured dynamometer forces. The error in the amplitude of the force estimation can be due to the estimation inaccuracy of the transmission ratio of the torque.

The similarity between the dynamic forces can be obtained by comparing the time and power spectral analysis of the signal. The comparison between the experimentally measured and estimated dynamic forces are shown in Fig. 9.21.

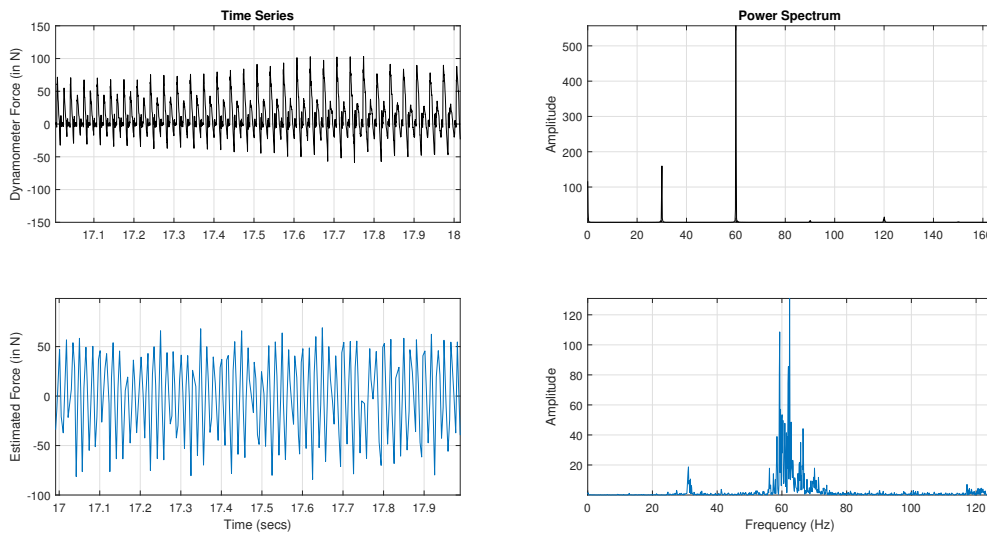


Fig. 9.21. Time and Power comparison between experimentally measured and estimated dynamic force

It can be observed that the power spectrum of the signals contain the same disturbance noises at 30 Hz and 60 Hz. Thus it can be said that the estimated forces are in agreement with the measured dynamometer force.

Using a Kalman filter based estimator

A Kalman estimator is used to compensate for the disturbances in the proposed system. The Kalman estimated cutting forces are compared with the dynamometer force to determine the accuracy of the force estimation.

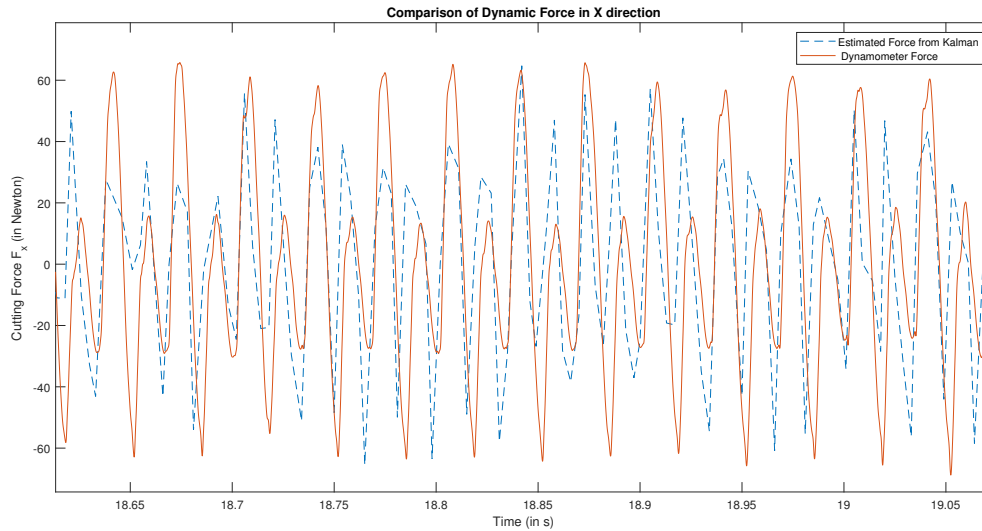


Fig. 9.22. Comparison between Kalman estimated and Dynamometer force

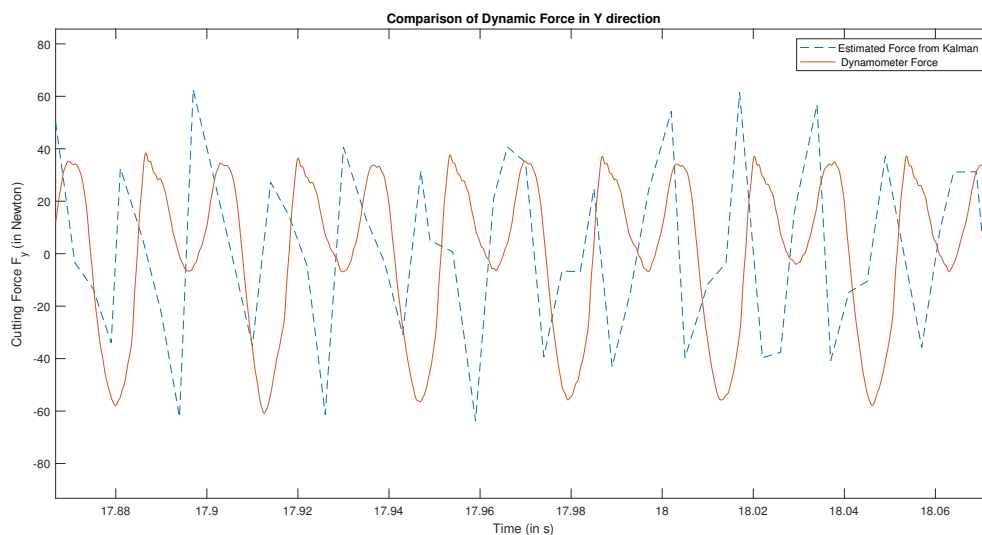


Fig. 9.23. Comparison between Kalman estimated and Dynamometer force

As seen from the Fig. 9.22 and Fig. 9.23, it is observed that the estimated force in X direction is in agreement with the measured dynamometer force. The deviation in estimation of force in the Y-axis can be attributed to the Y-axis carrying the A and B rotary drives of the CNC system.

The comparison between the dynamometer and the Kalman estimated forces are determined by plotting time and power series comparison of the cutting forces. The time and power series graphs for X, Y-axis are shown in Fig. 9.24 and Fig. 9.25 respectively.

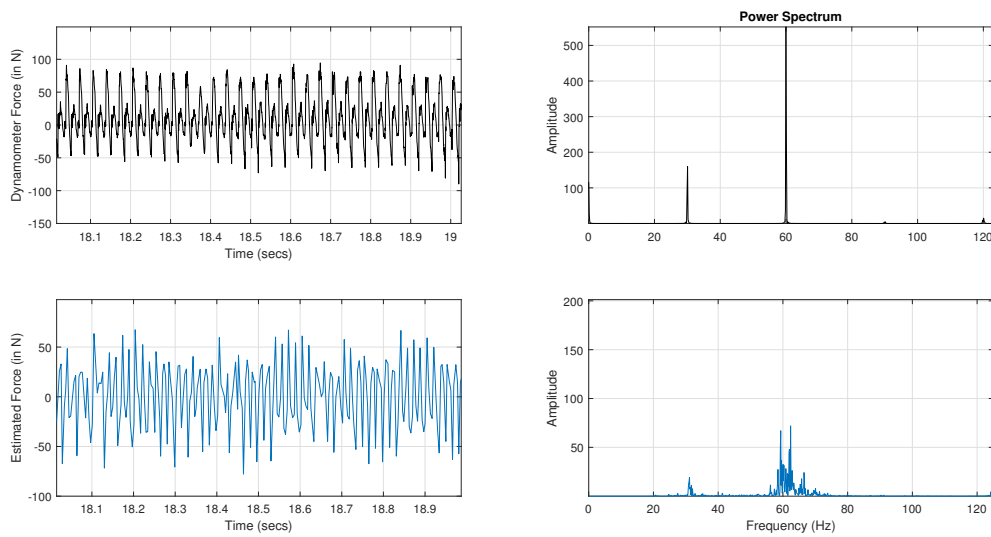


Fig. 9.24. Comparison between Kalman estimated and Dynamometer force for X-axis

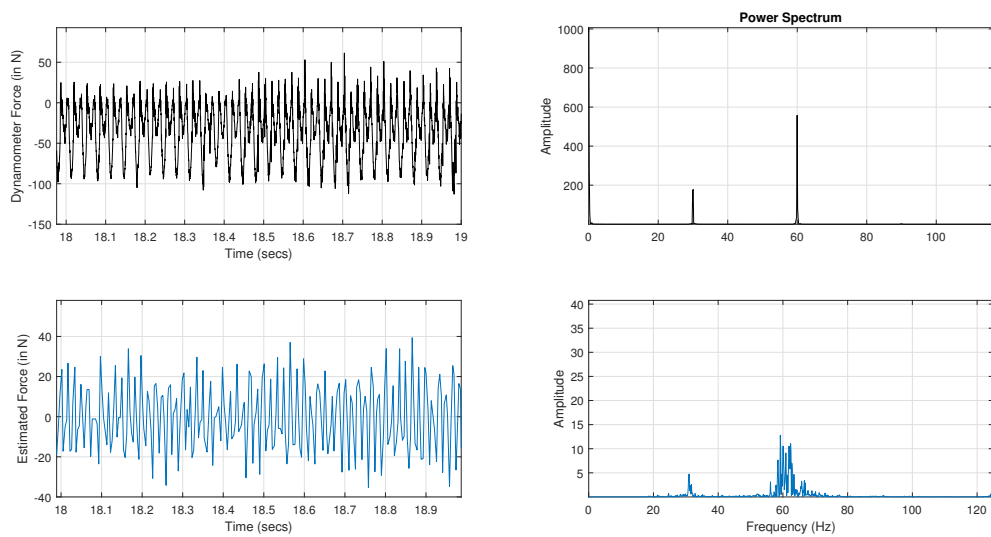


Fig. 9.25. Comparison between Kalman estimated and Dynamometer force for Y-axis

It can be observed from the power spectrum (Fig. 9.24 and Fig. 9.25) that the forces contain the same frequency components at 30 Hz and 60 Hz. Thus it can be concluded that the Kalman estimated forces are in good agreement with the Dynamometer forces.

To estimate the accuracy of the estimated forces, the amplitude between each section of the estimated Kalman forces and the dynamometer forces are compared and plotted in the Fig. 9.26.

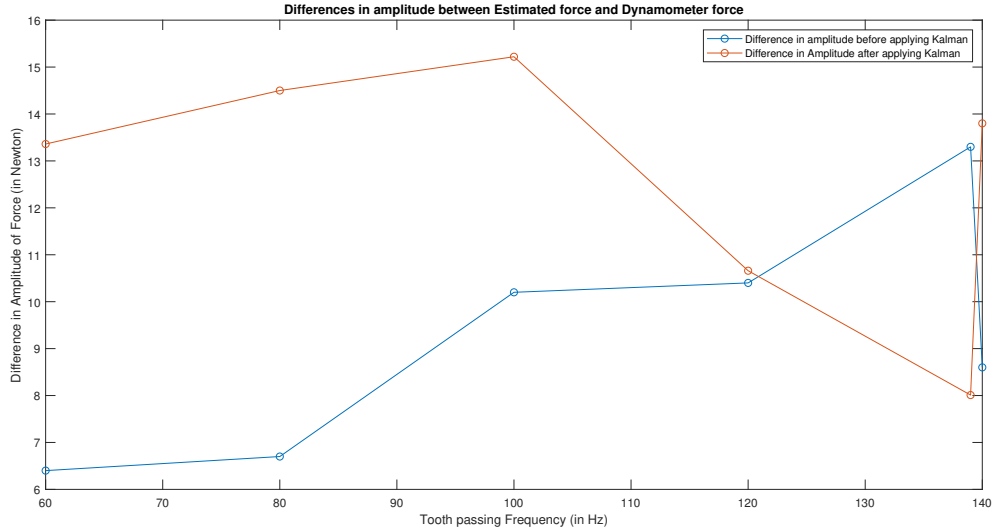


Fig. 9.26. Performance comparison before applying Kalman estimator and after Kalman estimator

The average amplitude difference of 10 N is observed between the dynamometer and estimated cutting forces. This high difference in cutting force is due to aliasing in the servo-motor signal, the manual calculation of transmission ratio (r_g) and transfer function of the feed drive system.

9.3 Summary

In this chapter, the validation of the proposed system model is determined by performing air cutting experiments and cutting operation on a work-piece. The static component of the estimated cutting forces are avoided due to the variable offset and drift in the servo-current signal. It is determined from the time and power series comparison that the dynamic component of cutting forces estimated from the proposed system are in good agreement with the cutting forces from the dynamometer measurement.

However the comparison between the amplitude of the estimated Kalman and dynamometer forces shows deviation in amplitude of the cutting forces (range of 10 N). The deviation in amplitude for the estimated value can be attributed to the aliasing in the signal, errors in system due to missing data points, manual computation of the transmission ratio and transfer function of the feed drive system. The conclusion and the approaches that can be applied to improve the master thesis work are presented in next chapter.

Chapter 10

Conclusion and Future Research

The master thesis work discusses an indirect and simple approach using Kalman filter for estimation of cutting forces from five axis CNC machining. The proposed model estimates the cutting force using the current measurement from the servo-drive of the CNC machine. Machining tests were designed and performed on the CNC machine to capture the machine dynamics of the five axis machine. The main conclusions derived from the master thesis work is summarized below:

- The reliability of the estimated cutting force depends on the accuracy of estimation of friction, inertia parameters and the black-box model which provides the transition from servo-torque measurements to the cutting force at the tool-tip of the machine.
- The frequency response from the servo-motor and cutting force is captured by performing machining tests using a sensorized hammer. The impact hammer tests and static load tests are designed to capture the structural and dynamic modes present in the CNC machine.
- A simple and generalized method for estimation of frictional torque components in the CNC machine is estimated using Coulomb and viscous friction model. As the estimation of the torque parameters varies with different CNC machines, specific air cutting tests are designed and performed to validate the estimated torque measurement.
- Similarly, a simple model for estimation of Inertial torque is presented in this thesis work by performing static load test on the CNC machine. The corresponding servo-motor response is curve fitted to find inertial parameters of the CNC machine.
- The servo-drive measurements are analysed in frequency to provide details in regards to the testing boundaries required to estimate the cutting force of CNC machine. It is determined from the servo-signals that the cutting force can only be estimated by running low speed machining tests due to the effect of aliasing of the signal.
- The transfer function of the rotary drives of the CNC system is avoided due to the inaccuracies and uncertain behaviour of the rotary drives. The direct measurement system, absence of worm-gear and high static behaviour also summate to the insufficient information of rotary drives.
- The errors present in the modelled black-box system is accounted due to inaccuracies present in the CNC system. One of the major error in the system is due to the variable and low sampling rate (250 Hz) of the CNC machine. Aliasing of the signal frequencies are induced in the modelled system if the tool performs cutting at tooth passing frequency higher than 250 Hz.

10.1 Suggestions for future works

The studies and the approach of the estimation of cutting force presented in the thesis work provides brief information regarding the machining tests, signal analysis and verification conditions for machining tests. The subjects to improve the master thesis work are recommended below.

- The methodology provided in the thesis work can estimate cutting forces when machining operations are stationary with low speed grade machining. To better estimate the cutting forces at dynamic high speed operations, an external precise accelerometer or displacement sensor can be attached to the spindle of the CNC machine.
- The geometry of the tool used for machining provides precise and better estimate of the cutting forces of different axis during the cutting operation with respect to the work-piece. However, the inclusion of kinematic model of the machine increases the complexity of the model.
- The precise measurement of disturbance transfer function of the CNC motor-drives is crucial to accurately estimate the cutting forces of the system. The inaccuracies observed in manually calculated transfer function can be avoided by real-time calibration of the transfer function parameters during the a designed cutting operation.
- The thesis work avoids modelling the rotary axis due to the lack of information regarding the static behaviour of the rotary drives. Modelling the rotatory axis of the CNC system can provide details when cutting operation performed in circular tool path during five axis machining.
- As the accuracy of the modelled system increases with complexity of the model, machine learning (ML) algorithms can be implemented to precisely measure the cutting forces from the CNC machine. The ML algorithms can be trained with machining data from different cutting operation to accurately estimate the tool-tip cutting forces.

Chapter 11

Appendix

X-axis Poles and Zeroes from Transfer function

Zeros	Poles
6.44215135935956e-07	-1.79883295530138e-06
-2.67873905731257e-07	2.74612047314887e-07
5.83042381884824e-06	1.77342053590714e-07
-4.08078039562582e-07	-9.91551024699259e-09
-4.48793365796201e-07	5.08912815137950e-08
-4.46415708418755e-07	-2.96078790705929e-08
-6.68075505020617e-07	-5.03015233017340e-08
8.99682055000267e-08	-3.06255695752902e-08
-1.59298767262192e-07	-6.82766141862311e-08
-6.38026067414941e-06	-9.76311693245771e-09
-6.51222590057638e-06	-3.47168689595084e-08
1.61907228072100e-05	-1.22965779895163e-07
-5.30741226048578e-06	-2.46827476920410e-08
2.88396653445352e-07	4.91410501436455e-08
-1.73614127292348e-06	6.00693013366983e-09
2.03984622975542e-06	1.19362820505009e-08
-2.24570334023337e-06	3.71422427062988e-09
-4.93832853548702e-06	2.10587782704185e-08
-3.54519996083168e-07	4.45027013451782e-08
-1.74815064568002e-05	7.24526232072857e-09
1.19441329671495e-05	3.92474415706689e-09
2.50545234379712e-05	-6.27596429744602e-07
0.000218147088530812	6.90940729588957e-07
-0.000222113314115826	-2.21102309223751e-07
-8.94944776398106e-06	-5.74830329450418e-09
2.80740593473417e-08	1.04970591520698e-11

Table 11.1: Poles and zeros of the obtained transfer function X-axis.

Y-axis Poles and Zeroes from Transfer function

Zeros	Poles
0.0218695938325274	0.0615391756495499
0.00142520914395177	-0.00757070189226879
0.156284426981795	-0.0172967235712783
0.0391739641191227	-0.00931739159268488
0.154217074322615	-0.000484918255804792
0.162536505536710	-0.00213801913608828
-0.0300751962455171	-0.00105139755230925
0.0326327770060196	-0.000383401522054600
0.0501785375945690	-0.00155626268966366
0.00806217497659361	-0.000576878018997594
0.0300025204384728	7.19519827010558e-05
-0.0163586214255455	0.000743250799568763
0.0782234829769165	-0.00113521728273782
0.0174569148886174	2.78609776468292e-05
0.0673889285359798	-0.000215961060155261
0.0735714581398463	9.50503618441548e-05
-0.00481262180868969	0.000296084316515586
0.0279040081187521	-0.000127812749065719
-0.0543602594858129	0.000506514925413446
0.0968278510972828	-0.000159508365895893
-0.0304260870954119	0.000397784421569113
0.108156562452844	0.000260343951580575
-0.0344304853574667	0.000319056537687505
0.135086082045967	-0.000167946903979586
0.00851755660541771	0.000225064126658402
0.0134307011433582	-0.000247076763728073

Table 11.2: Poles and zeros of the obtained transfer function Y-axis.

Z-axis Poles and Zeroes from Transfer function

Zeros	Poles
-0.0109770966349275	0.0416102694493669
0.0959561305274535	-0.0192148721719615
-0.125000256065395	-0.0121385673303319
0.105208037031703	-0.00867468086480535
-0.0863269198591566	0.00245447818503751
-0.0491976145447711	-0.000255422660092873
-0.00267394213928094	-0.000248747755694968
0.0122684878036696	-0.000928208598729511
0.000973935397498522	-0.000268704921041697
-0.0211347582577314	-0.000769503908331121
-0.00215849282851831	-0.00189261043757007
-0.0468759005682128	0.00103067708449080
0.0179375786846982	-0.000253874915640650
-0.0326536274091190	0.000472761091169750
0.0200641320788215	-4.94903486022360e-05
0.0123519381256710	-0.000138520866496328
0.00832114623191952	-4.13228781101663e-05
0.00106768374769995	-9.94419913668548e-05
-0.000221024604349916	4.01696703074683e-05
-0.000510050848894812	-9.43075599032735e-05
-0.00641378462451417	-5.47852162589167e-06
-0.0137878765578944	-7.94668624905352e-05
-0.00261774553690692	-2.39057035894255e-06
-0.0205745095976110	0.000115184383000886
0.00355188974903218	0.000118497833413441
0.00540536382166648	-8.20488077682671e-05

Table 11.3: Poles and zeros of the obtained transfer function Z-axis.

Bibliography

- [1] J. Luo, H. Ding, and A. Shih, “Induction-heated tool machining of elastomerspart 2: Chip morphology, cutting forces, and machined surfaces,” *Machining Science and Technology - MACH SCI TECHNOL*, vol. 9, 12 2005.
- [2] Y. Altintas and S. Park, “Dynamic compensation of spindle-integrated force sensors,” *CIRP Annals*, vol. 53, no. 1, pp. 305 – 308, 2004.
- [3] P. Albertelli, M. Goletti, M. Torta, M. Salehi, and M. Monno, “Model-based broadband estimation of cutting forces and tool vibration in milling through in-process indirect multiple-sensors measurements,” *International Journal of Advanced Manufacturing Technology*, 06 2015.
- [4] M. Xu, B. Cai, C. Li, H. Zhang, Z. Liu, D. He, and Y. Zhang, “Dynamic characteristics and reliability analysis of ball screw feed system on a lathe,” *Mechanism and Machine Theory*, vol. 150, p. 103890, 2020.
- [5] “Kistler multicomponent dynamometer 5 ... 10 kn, top plate 100x170 mm type 9257b,” no. 9257B₀00 – 151e – 07.18, 2009.
- [6] W. Kritzinger, M. Karner, G. Traar, J. Henjes, and W. Sihn, “Digital twin in manufacturing: A categorical literature review and classification,” *IFAC-PapersOnLine*, vol. 51, no. 11, pp. 1016 – 1022, 2018. 16th IFAC Symposium on Information Control Problems in Manufacturing INCOM 2018.
- [7] W. Luo, T. Hu, Y. Ye, C. Zhang, and Y. Wei, “A hybrid predictive maintenance approach for cnc machine tool driven by digital twin,” *Robotics and Computer-Integrated Manufacturing*, vol. 65, p. 101974, 2020.
- [8] D.-J. Cheng, J. Zhang, Z.-T. Hu, S.-H. Xu, and X.-F. Fang, “A digital twin-driven approach for on-line controlling quality of marine diesel engine critical parts,” *International Journal of Precision Engineering and Manufacturing*, 08 2020.
- [9] K. P. Monroy Vazquez, C. Giardini, and E. Ceretti, *Cutting Force Modeling*, pp. 315–329. Berlin, Heidelberg: Springer Berlin Heidelberg, 2014.
- [10] T. Ogedengbe, A. Okediji, Y. Abioduna Abideen, O. Aderoba, A. O.A., I. Alabi, and A. Oluwasanmi, “The effects of heat generation on cutting tool and machined workpiece,” *Journal of Physics Conference Series*, vol. 1378, pp. 1–10, 12 2019.
- [11] G. Byrne, D. Dornfeld, and B. Denkena, “Advancing cutting technology,” *CIRP Annals - Manufacturing Technology*, vol. 52, pp. 483–507, 01 2003.

- [12] B. Denkena and F. Flter, “Adaptive cutting force control on a milling machine with hybrid axis configuration,” *Procedia CIRP*, vol. 4, pp. 109 – 114, 2012. 3rd CIRP Conference on Process Machine Interactions.
- [13] C. Rao, D. N. Rao, and P. Srihari, “Influence of cutting parameters on cutting force and surface finish in turning operation,” *Procedia Engineering*, vol. 64, pp. 1405 – 1415, 2013. International Conference on Design and Manufacturing (IConDM2013).
- [14] E. Bohez, “Five-axis milling machine tool kinematic chain design and analysis,” *International Journal of Machine Tools and Manufacture*, vol. 42, no. 4, pp. 505 – 520, 2002.
- [15] “Cnc machine <https://www.thomasnet.com/articles/custom-manufacturing-fabricating/understanding-cnc-machining/>,”
- [16] J.-D. Kim and D.-S. Kim, “Development of a combined-type tool dynamometer with a piezo-film accelerometer for an ultra-precision lathe,” *Journal of Materials Processing Technology*, vol. 71, no. 3, pp. 360 – 366, 1997.
- [17] J. Kim, H. Chang, D. Han, D. Jang, and S. Oh, “Cutting force estimation by measuring spindle displacement in milling process,” *CIRP Annals*, vol. 54, no. 1, pp. 67 – 70, 2005.
- [18] D. V. Fritz Klocke, Stephan Kratz, “Position-oriented process monitoring in freeform milling,,” *CIRP Journal of Manufacturing Science and Technology*, vol. 1, pp. 103–107, 2008.
- [19] M. Rizal, J. A. Ghani, M. Z. Nuawi, and C. H. Che Haron, “Development and testing of an integrated rotating dynamometer on tool holder for milling process,” *Mechanical Systems and Signal Processing*, vol. 52-53, pp. 559 – 576, 2015.
- [20] M. Rizal, J. A. Ghani, M. Z. Nuawi, and C. Haron, “An embedded multi-sensor system on the rotating dynamometer for real-time condition monitoring in milling,” *The International Journal of Advanced Manufacturing Technology*, vol. 95, pp. 811–823, 2018.
- [21] Y. Altintas, “Prediction of Cutting Forces and Tool Breakage in Milling from Feed Drive Current Measurements,” *Journal of Engineering for Industry*, vol. 114, pp. 386–392, 11 1992.
- [22] Y.-H. Jeong and D.-W. Cho, “Estimating cutting force from rotating and stationary feed motor currents on a milling machine,” *International Journal of Machine Tools and Manufacture*, vol. 42, no. 14, pp. 1559 – 1566, 2002.
- [23] Z. Xie, Y. Lu, and J. Li, “Development and testing of an integrated smart tool holder for four-component cutting force measurement,” *Mechanical Systems and Signal Processing*, vol. 93, pp. 225 – 240, 2017.
- [24] D. Aslan and Y. Altintas, “Prediction of cutting forces in five-axis milling using feed drive current measurements,” *IEEE/ASME Transactions on Mechatronics*, vol. 23, no. 2, pp. 833–844, 2018.
- [25] A. Albrecht, S. S. Park, Y. Altintas, and G. Pritschow, “High frequency bandwidth cutting force measurement in milling using capacitance displacement sensors,” *International Journal of Machine Tools and Manufacture*, vol. 45, no. 9, pp. 993 – 1008, 2005.

- [26] R. P.-V. R. d. J. R.-T. W. L.-T. Luis Alfonso Franco-Gasca, Gilberto Herrera-Ruiz, “Sensorless tool failure monitoring system for drilling machines,” *International Journal of Machine Tools and Manufacture*, vol. 46, Issues 34,.
- [27] R. Koike, K. Ohnishi, and T. Aoyama, “A sensorless approach for tool fracture detection in milling by integrating multi-axial servo information,” *CIRP Annals*, vol. 65, no. 1, pp. 385 – 388, 2016.
- [28] Y. Altintas, A. Verl, C. Brecher, L. Uriarte, and G. Pritschow, “Machine tool feed drives,” *CIRP Annals*, vol. 60, no. 2, pp. 779 – 796, 2011.
- [29] S. Kim, “Moment of inertia and friction torque coefficient identification in a servo drive system,” *IEEE Transactions on Industrial Electronics*, vol. 66, no. 1, pp. 60–70, 2019.
- [30] Y. Liu, J. Li, Z. Zhang, X. Hu, and W. Zhang, “Experimental comparison of five friction models on the same test-bed of the micro stick-slip motion system,” *Mechanical Sciences*, vol. 6, pp. 15–28, 03 2015.
- [31] S. Andersson, A. Sderberg, and S. Bjrklund, “Friction models for sliding dry, boundary and mixed lubricated contacts,” *Tribology International*, vol. 40, no. 4, pp. 580 – 587, 2007. NORDTRIB 2004.
- [32] K. Johanastrom and C. Canudas-de-Wit, “Revisiting the lugre friction model,” *IEEE Control Systems Magazine*, vol. 28, no. 6, pp. 101–114, 2008.
- [33] D. Stephenson and J. Agapiou, “Metal cutting theory and practice.,” 2016.
- [34] H. Kull Neto, A. E. Diniz, and R. Pederiva, “Influence of tooth passing frequency, feed direction, and tool overhang on the surface roughness of curved surfaces of hardened steel,” 2016.
- [35] D. Simon, “Optimal state estimation: Kalman, h, and nonlinear approaches,” 01 2006.
- [36] “Iot implementation of kalman filter to improve accuracy of air quality monitoring and prediction.,” 2019.
- [37] P. Kalata and S. L. Fagin, “Kalman filtering: One form fits all - an innovative, pure square root process,” in *1990 American Control Conference*, pp. 2959–2964, 1990.
- [38] M. Zawada-Michaowska, P. Pieko, J. Jzwik, L. Stanisaw, D. Mika, and J. Pytka, “Uncertainty estimation of measuring circuit during cutting forces measurement using the piezoelectric dynamometer,” in *2020 IEEE 7th International Workshop on Metrology for AeroSpace (MetroAeroSpace)*, pp. 441–445, 2020.
- [39] F. Esqueda, V. Vlimki, and S. Bilbao, “Aliasing reduction in soft-clipping algorithms,” in *2015 23rd European Signal Processing Conference (EUSIPCO)*, pp. 2014–2018, 2015.
- [40] L. Lévesque, “Revisiting the nyquist criterion and aliasing in data analysis,” *European Journal of Physics*, vol. 22, pp. 127–132, feb 2001.
- [41] P. Vandewalle, L. Sbaiz, J. Vandewalle, and M. Vetterli, “How to take advantage of aliasing in bandlimited signals,” in *2004 IEEE International Conference on Acoustics, Speech, and Signal Processing*, vol. 3, pp. iii–948, 2004.

- [42] S.-S. Yeh and H.-C. Su, “Development of friction identification methods for feed drives of cnc machine tools,” *The International Journal of Advanced Manufacturing Technology*, vol. 52, pp. 263–278, 05 2011.
- [43] “Power spectrum <https://www.mathworks.com/help/dsp/ug/estimate-the-power-spectrum-in-matlab.html>: :text=theno. 9257B000 – 151e – 07.18.